EUROPEAN COMMISSION
RESEARCH EXECUTIVE AGENCY

“ECO DRIVE”

Noise and vibration in eco-efficient powertrains

H2020 FRAMEWORK PROGRAMME

Marie Skłodowska Curie European Training Network (ETN)

Grant Agreement 858018

D4.4
Mid-term public technical report WP4

Deliverable no.	D4.4
Dissemination level	Public
Work Package	WP4
Author(s)	All
Co-author(s)	
Status (F: final, D: draft)	F
File Name	ECO_DRIVE_D4.4.pdf
Project Start Date and Duration	March 1st, 2020 – February 29, 2024

This document reports on the status at mid-term (M24) of ECO DRIVE regarding the research activities developed within WP4 *NVH analysis of lightweight transmission systems and drivelines.*

The document is structured according to the 3 tasks within the WP:

- Task 4.1: Torsional vibration analysis.
- Task 4.2: Analysis of gear and bearing contact forces and strains.
- Task 4.3: Analysis of transmission-induced vibrations and noise.

EUROPEAN COMMISSION
RESEARCH EXECUTIVE AGENCY

“ECO DRIVE”

Noise and vibration in eco-efficient powertrains

H2020 FRAMEWORK PROGRAMME

Marie Skłodowska Curie European Training Network (ETN)

Grant Agreement 858018

Torsional vibration analysis

Deliverable no.	
Dissemination level	
Work Package	WP4
Author(s)	Steve Koshy Mathew (ESR4)
Co-author(s)	
Status (F: final, D: draft)	F
File Name	
Project Start Date and Duration	March 1st, 2020 – February 29, 2024

Contents

Acronyms **1**

1 Abstract **2**

2 Introduction **3**
2.1 Electric drive Multi-physics Modelling 4

3 Angular modelling technique **5**

4 Modelization of jefcott rotor **6**
4.1 Introduction 6
4.2 General Model description 7
4.3 Kinematics of rotating element 8
4.4 Overall dynamic equation of the rotor 9
4.5 Results 10
4.5.1 Comparison of the results between gyroscopic and non gyroscopic models 10

5 Bearing Modelling **13**
5.1 Introduction 13
5.2 General Model description 13
5.3 Results 14

6 Conclusion **16**

A Apendix Numerical Simulation data **17**

Bibliography **20**

List of Figures

1 Electric Drive-line multi-physics model 4
2 Time domain analysis 6
3 Angular domain analysis 6
4 Jefcott Rotor Bearing Model 8
5 Euler angle coordinate system 8
6 Spectral plot for Non Gyroscopic model 11
7 Spectral plot for Gyroscopic model 11
8 Campbell Plot-Gyroscopic model 12
9 Campbell Plot- Non Gyroscopic model 12
10 Frequency plot 15
11 Frequency plot without eigen modes 15
12 Bearing A Force plot 15
13 Zoomed View 15
14 IAS of the Shaft 16
15 Zoomed View 16

List of Tables

1 Properties of the system. 17

Acronyms

BPFO Ball Pass frequency outer.

FEA Finite Element Analysis.

IAS Instantaneous angular speed.

ICE Internal combustion engine.

NVH Noise Vibration and Harshness.

1 Abstract

Electrification of vehicle has radical changed how Noise Vibration and Harshness (NVH) performance of a vehicle is perceive due to introduction of tighter NVH constraints. High-speed electrical engines are now been used to achieve very large range of speeds, leading to non-stationary operating conditions. Therefore, predicting accurately the non-stationary loads and deformations during these transient regimes is of first importance for a correct design. In this report, we demonstrate a novel way of building a dynamic model for high-speed rotors under the assumption speed is not considered to be constant as seen in majority of the literature. For this purpose, a coupled dynamics model of the Jeffcott rotor was developed using angular modelling approach. Euler angle transformation was used in building the model and some observation regarding the differences due to non-symmetric nature of the equations are discussed. Then, the general framework of a rotor-bearing system will be the support used to illustrate this approach.

Keywords: Angular Modelling, Instantaneous Angle Speed, Jeffcot Rotor system, Bearing modeling

2 Introduction

Electric Mobility has grown its importance in industry specifically in automotive, from the inclusion of environmental and energy regulations laid out in United Nations Climate Change Conference held in Paris in 2015 [1]. The essence of electric and hybrid vehicles is also triggered by their adherence to NVH features. Experimenting with NVH prediction for such machines is expensive, and it also gives very limited access to the design attributes of the entire assembly. And Simulation models have always been used to deepen the understanding of the physical phenomena.

The research will focus on the first steps of the research activities started in the framework of the project "ECO-DRIVE[1]" funded by the H2020 MSCA ITN program. This project develops new technologies for the testing and simulation of eco-powertrains, addressing the complex challenges related to its NVH performance. The aim of the project is to develop a generalized model of a complete transmission line from the engine to the wheels. The model will use the experimental measurements on a transmission test rig or vehicle in order as the benchmark especially in non-stationary conditions in order to calibrate the torsional and non-linear parameters, to define the best location for angular measurements. After calibration, the model will be used to study the improvements in the driveline design by adding passive or active damping components. The angular approaches suggested in both the experimental and simulation research activities will also lead to a new path for drive-transmission characterization (cyclic sources and mechanical transfer paths) through angle-time analysis tools with alternative signals like angular speed, position, vibration and current.

The initial studies will be focused on the interactions between the magnetic and mechanical phenomenon of an electrical light transmission with mechanical components like bearings, gears and electrical machine, with main focus on couplings like gyroscopic effects and operates in non-stationary conditions. Using a Jeffcott model, the mechanical model is studied under various stationary conditions and non-stationary conditions using angle domain analysis. By using this model, a parametric study is proposed to analyze the effects of different parameters like rotational damping, bearing stiffness and damping with respect to the performance of the model under different conditions. The construction of a mechanical model is intended to be used as a tool to develop and test complex drive line systems in a controlled environment in which the severity of the defect may be analyzed related to the operating conditions of the machine. With the interest of developing this research opportunities, LaMCoS decided to propose the current thesis subject with a funding of the ECO DRIVE in a H2020 MSCA framework.

The following sections provide an overview of the above mentioned angular modelling techniques in terms of application used in bearing applications in a simple jeffcott rotor system.

[1] `https://h2020-ecodrive.eu/`

2.1 Electric drive Multi-physics Modelling

An electric vehicle contains an electric driveline which consists of a electric motor and a gear train. As we know, there are many advantages in using an electric powertrain over traditional internal combustion engine ICE. But NVH characteristics of an electric powertrain is important factor during the design of the system because of its contribution to overall cabin noise during acceleration and deceleration. The experimental prediction of NVH characteristic of complex drive train is expensive and time consuming. Since of these restrictions, computer simulation technology is becoming more widely used because it has progressed to the point where it can provide detailed information to designers for this multi-physics phenomenon connected to the system.
Rotating components with a discrete periodic geometry (electrical engine, gears, bearings, timing belts, etc.) generate cyclic excitations that can be efficiently described in the multi-physics modelling.These excitations are in interaction through various structual components which are in rotation or in rest (shaft, bearing , gears, motors). The general modelling approach is based on the modelling description with connecting elements as shown in (Figure 1)

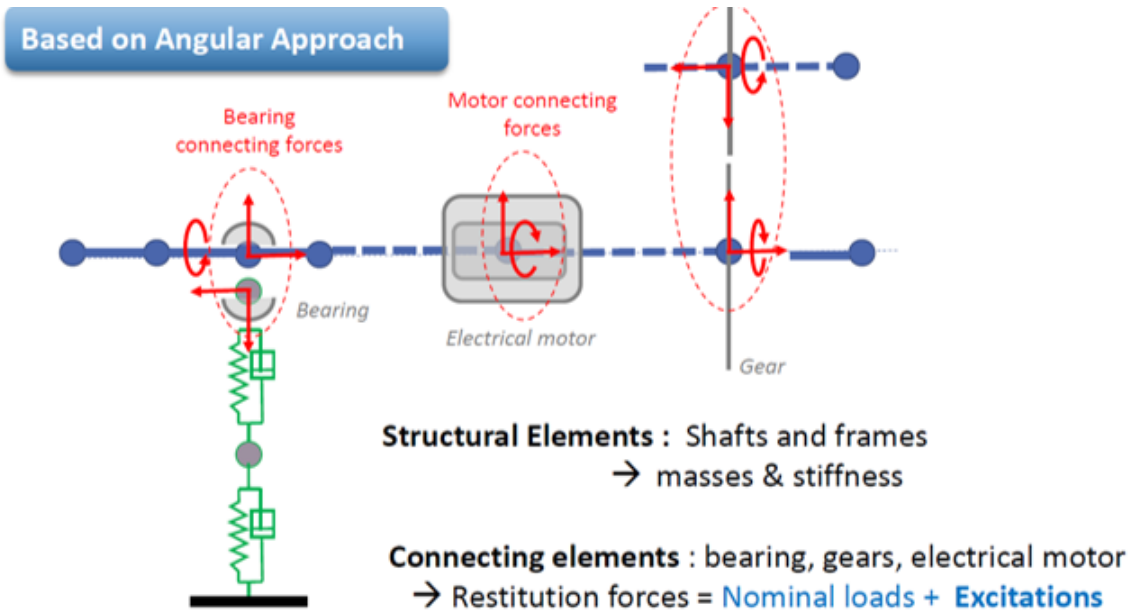

Figure 1: Electric Drive-line multi-physics model

There has been lot of recent numerical simulation attempts to simulate different elements in the drivetrain for ex. a motor or a gear train for NVH studies. [2] built models to simulate the acoustic radiation of a switched reluctance motor of the electrical machine using finite element. [3] developed multi physics simulation environment which was used for radial forces and sound pressure evaluation of a permanent magnet synchronous machine for light traction. [4] developed a statistical model for gears noise prediction in gearbox applications. [5] stuided the effects of transmission error and bearing preload on gearbox noise. While these studies and models help us understand the physical attributes of vari-

ous phenomenon occuring in each individual element of a drivetrain, it fails to capture the combination effects of elements in the system and their coupling with the global rotation of the machine. Few studies have tried to integrate both motor and geartrain performed structural simulation using FEA ([6], [7] and [8]). However, all the models are built under the assumption the rotating speed is constant but as we know rotating speed of machine varies due to mechanical behaviour of elements,e.g due to the BPFO of bearing. This is the premise of the modelling that has been in done in our work. Using the angular modeling technique, we built models which do not have assumption on rotating speed being constant and also coupling different elements using multi-physics approach to make global analysis of a electric drivetrain.

3 Angular modelling technique

The section is dedicated to parametric analysis of a rotating system with two degrees of freedom (d.o.f) in time and angular domains. The study is to show the advantages and limitations of using angular modelling technique over time domain analysis.
Time domain modelling follows the traditional approach, in which, all the variables are measured and analyzed with respect to time depending upon the application. This is especially used in the model-based methods for fault detection and condition monitoring.[9], [10]. But many a times, time/frequency analysis cannot track the faulty condition prevalent in the system [9]. The use of instantaneous angular speed (IAS) to evaluate faults in rotating machines has become a more common in all industrial applications [10]. [11]investigated the faults in diesel engine through IAS . They utilized IAS to monitor the condition of electric motor, as this is particularly useful in getting the exact angular position of the fault. This led to the modelling the system in angular domain, in which motion equations translated into angular domain.This approach stresses out the need to know precisely the relationship between time and angular position of the rotating part. So, in this chapter a rotating system is modelled using time and angular model approach and compared with each other. Mathematically t is expressed as in Equation 1 in terms of function of the angular position

$$T = \varphi(\theta) \tag{1}$$

We assume $\varphi(\theta)$ to be bijective.
A simplified mathematical model of a two d.o.f rotating system was developed to illustrate the feasibility of angular modelling technique. An cyclic perturbation was introduced to the system to study in both angular and time domain. The analysis of the rotating speed in angular domain Figure 2 highlights the angular periodicity of the perturbation that appears as a peak for the value at 5.71. This is due to the fact that the kinematics of excitation was set to 5.71 to test the accuracy. On the other hand, through time domain analysis of the signal in Figure 3, we observe excessive fluctuations in speed which makes the actual fault to be inconceivable, as we can see small variations in speed till 80 Hz.

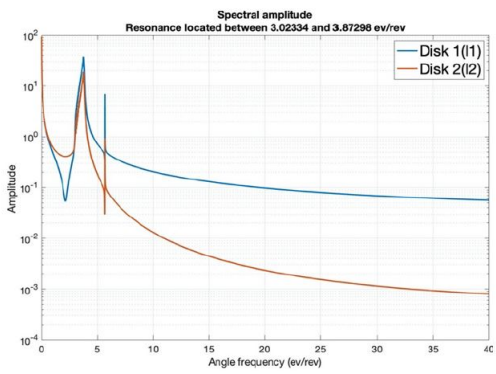

Figure 2: Frequency Response in Time domain

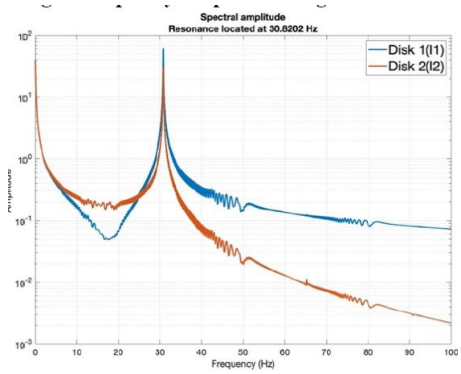

Figure 3: Frequency Response angular domain

The angular modelling technique is quite a simple and elegant solution to identify exact periodic excitations in a rotating system as shown above, so key takeaway from this exercise is,

1. Temporal sampling is not able to locate and identify cyclic perturbation.
2. Angular Model is more robust and adequate to investigate angularly periodic excitations
3. Numerical models allow evaluating the smallest amplitude of the perturbation that could be detected in the signal analysed.

4 Modelization of jefcott rotor

4.1 Introduction

The last section , a general introduction of the angular modelling technique was presented and getting into the specifics of the advantages of using angular modelling technique over time domain analysis. Through this section, the proposed approach is used to explain how mechanical rotor system behaves due to the system dynamics. This is realized by introducing a Jeffcott rotor bearing model with a rigid shaft, rigid disk and supported by bearings with constant stiffness and damping. The proposed approach is tested by the Jeffcott model architectures and some simulations are compared with experimental results available in the literature. At the end of the chapter the discussion of the results will be presented leading to the integration of the model into more complex mechanical configurations.
Instantaneous angular speed is now widely used in fault diagnosis and condition monitoring in rotating machines. The evolution of advance sensor technology such as magnetic and optical encoders helped to us get accurate predictions of the IAS of a rotating machine which is especially useful in automotive industry. One such example is given in [12], which proposed approach to detect and quantify rattle noise in automotive gearboxes operating under non-stationary conditions by means of vibration or instantaneous angular speed measurements.Using Jefcott rotor model, we can easily understand system behavior under faulty

conditions[13] ,[14], [15]. In order to accurately prediction the system behavior, one must take care of the assumption used in the models. The rotor or the shaft can be considered as rigid or flexible or the inclusions of the gyroscopic effects in the system.
One of the key assumptions in the study of dynamic analysis of rotors is the assumption of constant rotational speed. This is not helpful when we want to understand the dynamic behavior of the mechanical in the transient regime. It is evident from the [16] [17] that non-linearities from the shaft acceleration is modelled by assumption of constant speed. So it is important to realize that the dynamic model based on a given speed of rotation, whether the latter is constant or not, presume dealing with an ideal power supply with the described speed increase or decrease. Second important phenomenon is the influence of gyroscopic effect on the rotor system. [18] proposed a model of an unbalanced rotor with assumption of gyroscopic effect being neglected for the study of coupled torsional and lateral vibrations. [19] investigated the problem of bisynchronous torsional vibrations in rotating shafts and concluded that gyroscopic coupling term plays a more important role in the dynamic behavior of the shaft. By introducing this academic system, the main purpose is to show that the suppressing constant speed assumption may change the model classically used in the literature.
In this section, an example of jeffcott fully coupled model is proposed for the evaluation of the dynamic behaviour of rotors with gyroscopic effect and with the less restricting assumptions. Only the simplifying assumption of rigid disk is kept so that the focus is placed mainly to the bending-torsional coupling. Five degrees of freedom are defined for the system. A comparison study is done for various operating conditions such as stationary and non-stationary, with and without gyroscopic effects etc. to understand how the dynamics of system works with the Euler angle transformation modelling.

4.2 General Model description

The dynamic model of a rotor made of a rigid shaft, rigid disk and supported by flexible bearings with constant stiffness and damping will be explained in the following section (Figure 4). A mass unbalance is introduced to the system by adding it in the disk as cyclic excitation. The disk is considered to the asymmetric to the shaft center. The dynamic model is built using the Lagrange approach. An analysis of the impact of the different assumptions on the equations of motion of each component of the rotor is explored.

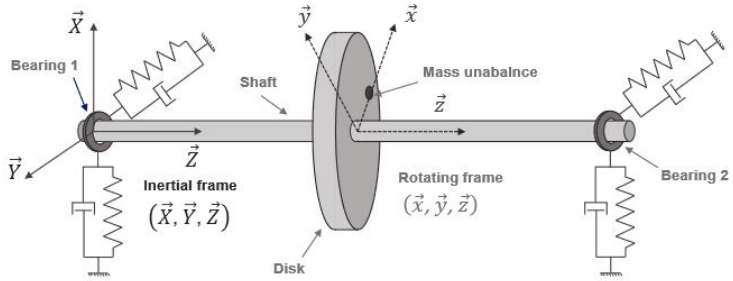

Figure 4: Jefcott Rotor Bearing Model

4.3 Kinematics of rotating element

The motion of the rotating shaft , in three-dimensional motion, can be completely described using Euler's angles defined via three successive rotations to specify the relations between the principal axes of the rotating frame (xyz) and the fixed frame (XYZ) as shown in (Figure 5). The system can be transformed by 1) rotating the system , parallel to fixed coordinates, into a deflected mode by an angle ϕ about the Z-axis 2) rotating the intermediate axes by an angle θ about the new X'- axis 3) rotating intermediate axes by an angle ψ about the z'-axis to produce the principal coordinates. The three angles ϕ, ψ and θ leading to three transformations are defined as Euler angles used by [20].

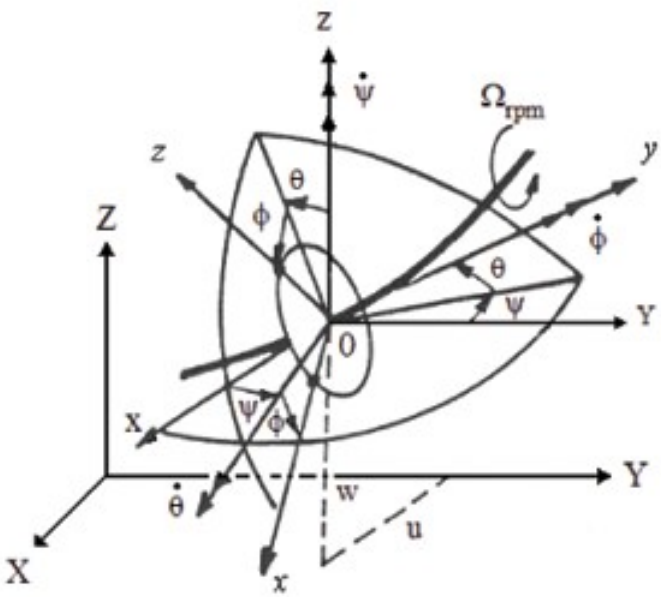

Figure 5: Euler angle coordinate system

The angular displacement about the X and Y axis are calculated using Euler angles as follows.

$$\theta_x = \theta.cos(\phi), \theta_y = \theta.sin(\phi) \tag{2}$$

The spin angle about the Z axis is defined by,

$$\phi = \theta + \psi \tag{3}$$

One can express the components of angular velocity in the direction of the principle axis as follows.

$$\omega_x = \dot{\varphi}_x \cos\varphi_y \cos\theta + \dot{\varphi}_y \sin\theta \tag{4}$$

$$\omega_y = -\dot{\varphi}_x \cos\varphi_y \sin\theta + \dot{\varphi}_y \cos\theta \tag{5}$$

$$\omega_z = \dot{\theta} + \dot{\varphi}_x \sin\varphi_y \tag{6}$$

4.4 Overall dynamic equation of the rotor

Given the study detailed above, the equations of motion overall system, under the assumed assumptions, are given by,

$$([M] + [k_d] + [M_u(\dot{\theta})])\ddot{q} + ([c] + [G_d(\dot{\theta})])\dot{q} + ([k])q = F^{coup} - F^{ext} \tag{7}$$

where F^{coup} represents a vector assembled with the coupling forces due to the gyroscopic effect and F^{ext} is the external load.

The equations of motion can be written by,

$$m\ddot{u} = 2k_x u + 2k_x (b-a)\,\varphi_y + 2c_x\dot{u} + c_x (b-a)\,\dot{\varphi}_y + f_x \tag{8}$$

$$m\ddot{v} = 2k_y v - 2k_y (b-a)\,\varphi_x + 2c_y\dot{v} - c_y (b-a)\,\dot{\varphi}_x + f_y \tag{9}$$

$$I_d\ddot{\varphi}_x + I_p\ddot{\theta}\dot{\varphi}_y = I_p\dot{\theta}\dot{\varphi}_y - k_y\varphi_x\left(a^2+b^2\right) + k_y v\,(b-a) + 2c_y\dot{\varphi}_x\left(a^2+b^2\right) - c_y\dot{v}\,(b-a) \tag{10}$$

$$I_d\ddot{\varphi}_y = -I_p\dot{\theta}\dot{\varphi}_x - k_x\varphi_y\left(a^2+b^2\right) - k_x u\,(b-a) + 2c_x\dot{\varphi}_y\left(a^2+b^2\right) + c_x\dot{u}\,(b-a) \tag{11}$$

$$I_p\ddot{\theta} + I_p\ddot{\varphi}_x\dot{\varphi}_y = I_p\dot{\varphi}_y\dot{\varphi}_x - C\dot{\theta} + T \tag{12}$$

where,

$$[M] = \begin{bmatrix} m & 0 & 0 & 0 & 0 \\ 0 & m & 0 & 0 & 0 \\ 0 & 0 & I_d & 0 & 0 \\ 0 & 0 & 0 & I_d & 0 \\ 0 & 0 & 0 & 0 & I_p \end{bmatrix}$$

$$[k_d] = \begin{bmatrix} 0 & 0 & 0 & 0 & 0 \\ 0 & 0 & 0 & 0 & 0 \\ 0 & 0 & 0 & 0 & I_p\dot{\varphi}_y \\ 0 & 0 & 0 & 0 & 0 \\ 0 & 0 & I_p\dot{\varphi}_y & 0 & 0 \\ & & & & \end{bmatrix}$$

$$[G_d] = \dot{\theta} \begin{bmatrix} 0 & 0 & 0 & 0 & 0 \\ 0 & 0 & 0 & 0 & 0 \\ 0 & 0 & 0 & I_p & 0 \\ 0 & 0 & -I_p & 0 & 0 \\ 0 & 0 & 0 & 0 & 0 \end{bmatrix}$$

$$F_{cou} = I_p \begin{bmatrix} 0 \\ 0 \\ 0 \\ 0 \\ \dot{\varphi}_x\dot{\varphi}_y \end{bmatrix}$$

$$F_{ext} = \begin{bmatrix} F_x \\ F_y \\ 0 \\ 0 \\ T \end{bmatrix}$$

$$K = \begin{bmatrix} 2k_x & 0 & 0 & 2k_x\,(b-a) & 0 \\ 0 & 2k_y & -2k_y\,(b-a) & 0 & 0 \\ 0 & -k_y\,(b-a) & k_y\left(a^2+b^2\right) & 0 & 0 \\ k_x\,(b-a) & 0 & 0 & k_x\left(a^2+b^2\right) & 0 \\ 0 & 0 & 0 & 0 & 0 \end{bmatrix}$$

$$C = \begin{bmatrix} 2c_x & 0 & 0 & c_x\,(b-a) & 0 \\ 0 & 2c_y & -c_y\,(b-a) & 0 & 0 \\ 0 & -c_y\,(b-a) & 2c_y\left(a^2+b^2\right) & 0 & 0 \\ c_x\,(b-a) & 0 & 0 & 2c_x\left(a^2+b^2\right) & 0 \\ 0 & 0 & 0 & 0 & C \end{bmatrix}$$

4.5 Results

4.5.1 Comparison of the results between gyroscopic and non gyroscopic models

The model is run in two conditions. First, the model includes the gyroscopic effects in the equation and in the next run, those effects are excluded. All other parameters are kept same for both conditions. Both simulations are run in non stationary conditions (speed ramp up). The rotational speed is increased from 20 $\mathrm{rad\,s^{-1}}$ to 1050 $\mathrm{rad\,s^{-1}}$. The graph in the next figure shows the Frequency Response of both simulations.

In both the simulations, the peak frequencies for both the gyroscopic and non gyroscopic simulation are at 81 Hz.(Figure 6 and Figure 7). But it is to be noted that the amplitude of peak frequencies in X and Y axis in gyroscopic simulation are different (Figure 7). This should not be the case, as the system is symmetric in both X and Y axis i.e the spring stiffness and damping are same in X and Y directions.
This behaviour is attributed to the use of Euler angles for the transformation of rotation.The non-symmetric nature of equations can be seen in eq. 10 and eq. 11.There is an extra term $(I_p\ddot{\theta}\dot{\varphi}_y)$ in the equation attributed to φ_x which is not present in equation attributed to φ_y.And the displacements in X and Y are dependent on φ_x and φ_y which is shown in eq. 8 and eq. 9.It is also to be noted that this extra term $(I_p\ddot{\theta}\dot{\varphi}_y)$ which is proportional to the rotational acceleration and does not exist when constant speed assumption is taken into account.

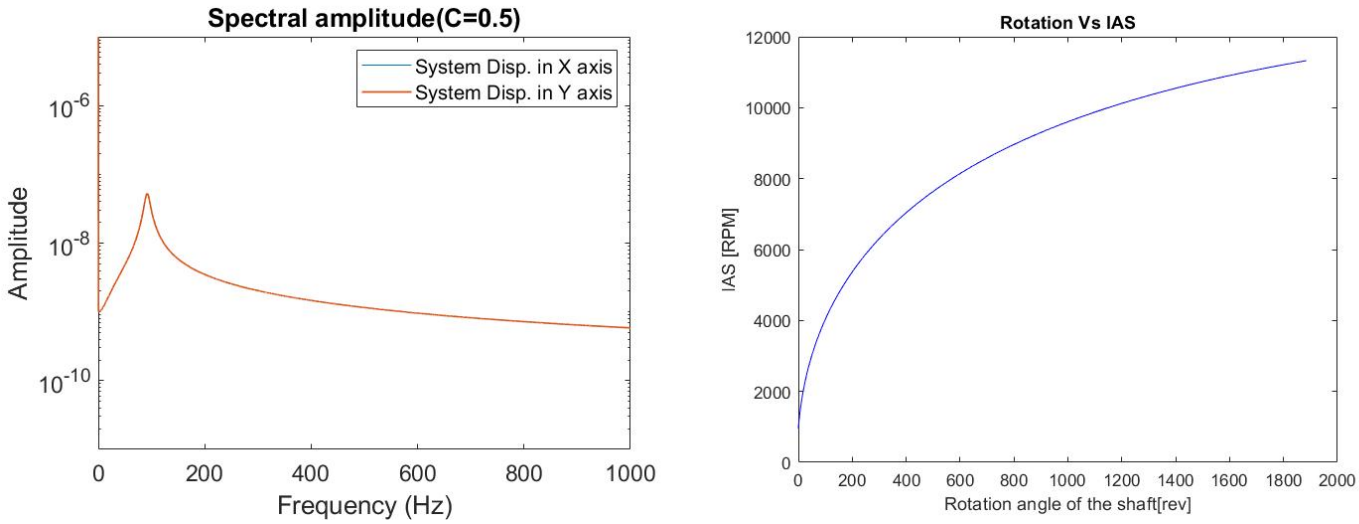

Figure 6: Spectral plot for Non Gyroscopic model

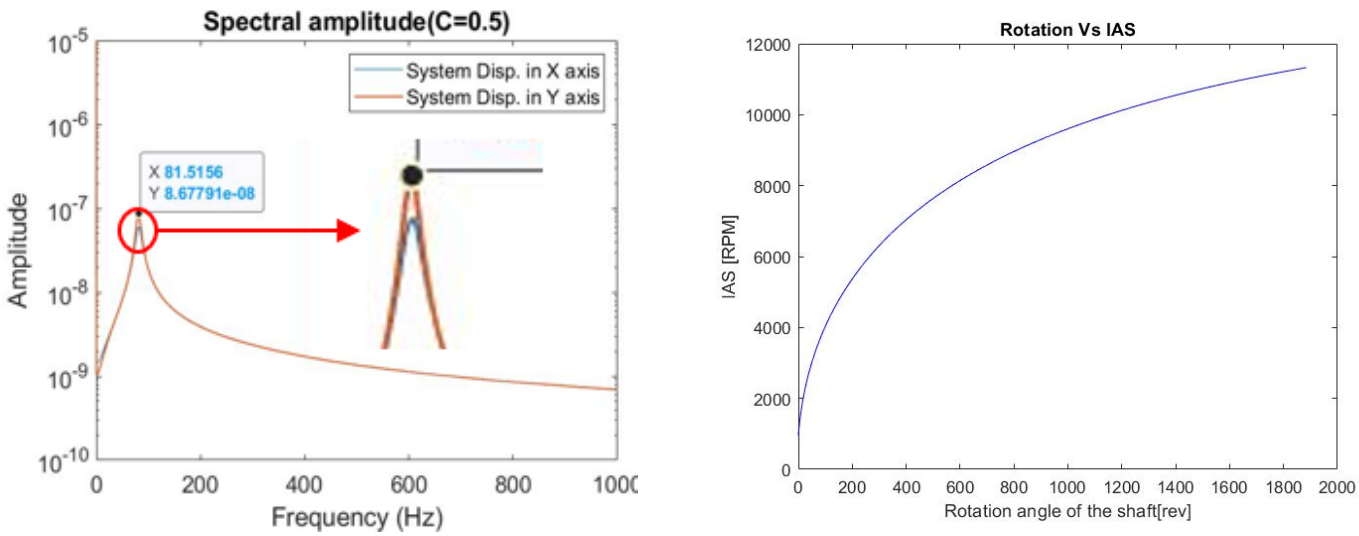

Figure 7: Spectral plot for Gyroscopic model

The Campbell diagram of this rotor is plotted for the two cases (gyroscopic and non gyroscopic conditions) as seen in Figure 8 and Figure 9.

The eigen frequencies are plotted are in the Campbell plots with respect to the rpm. The results in the gyroscopic model (Figure 8) shows that there are 4 eigen modes.Typical, that natural frequency of the 1st order is not affected by rotational speed, while the 2nd order shows obvious difference between the forward and backward whirling motion. But in case of gyroscopic results, one can clearly see that there is mode splitting happening in the 1st order as speed increases. At higher speed, the split is more evident. This behaviour is also attributed the use of Euler angles for the transformation of rotation as discussed above.This is not seen in the case of non gyroscopic results as seen in (Figure 9).

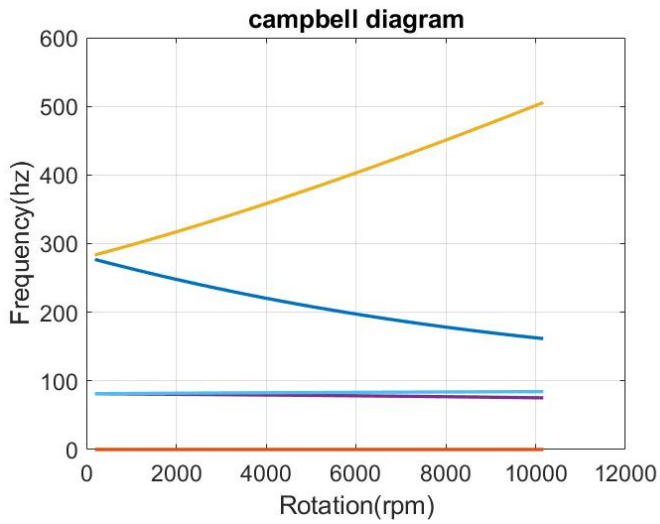

Figure 8: Gyroscopic

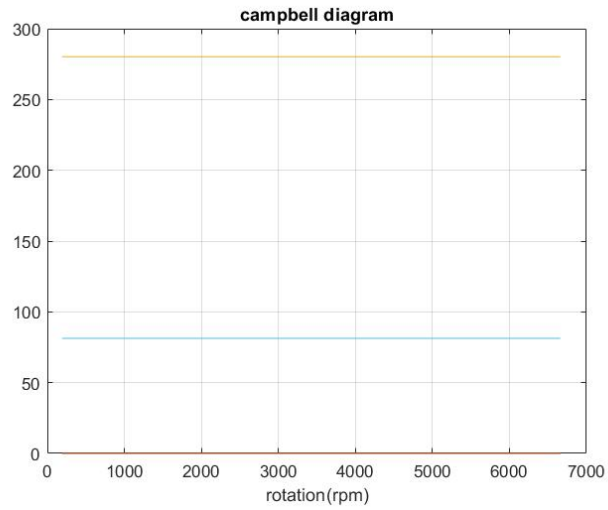

Figure 9: Non-Gyroscopic

The analysis presented in this section to describe a simple jeffcott model to study the system behavior for various parameters under different stationary and non- stationary conditions. The conclusions are summarised as follows.

1. When gyroscopic effects are introduced into the system, there are small variations in the amplitude X and Y axis.

2. there was splitting of the 1st and 2nd mode in eigen frequencies, and this effect is more prominent as we increase the rotational speed / decrease the rotational damping of the system when gyroscopic effects are introduced

Both this phenomenon has been attributed to use of using Euler angles leads to a non symmetric set of equation where φ_x and φ_y don't have same weight. Further studies will be carried out for more complex system such as non linear bearing models, non stationary input condition from electric motor before implementation to entire driveline of a vehicle.

5 Bearing Modelling

5.1 Introduction

This section the same angular modelling approach is used to explain how torque variations are induced into the shaft of a mechanical system by means of the roller element bearing dynamics and load variations. This shows us how , speed should not be considered constant in the simulation models.The example is an simple model which does not describe the perturbations or faults in bearings leading to the angular speed variations.
Rotating shafts has been used in almost all the industrial machines such as steam and gas turbines, turbo generators and ICE . Therefore, it is necessary to investigate the behavior of these systems under various operating situations, particularly when there are vibrations on the bearing base. Bearing and housing must be designed to be resilient to critical speeds and also be resilient to vibration caused by gyroscopic movements or centrifugal force as in case of aircraft, because damages to bearing can cause catastrophic failures. There have been numerous studies on the topic, the dynamic response of geared rotor-bearing systems. Some of them were based on experimental response of the bearing while others were based theoretical analysis of mechanical component failures. One of the interesting work on this , was done by [21] in which bearing dynamics was described in terms of time frequency equations, taking into account the kinematics of the bearing leading to the characteristic frequencies. Recent models use the theory of Hertz [22] for the estimation of the non linear normal force between the rolling elements and the race. This demonstration shows how we can couple the model into more complex mechanical architectures. Among the novelties introduced, the model is suitable to manage variable operating conditions by considering the angular degree of freedom leading to the construction of the angle-time function and also the approach is the integration of the rolling resistance phenomenon describing the introduction of the perturbation leading to angular perturbations originated by the roller bearing dynamics.

5.2 General Model description

To achieve the aim of making the model, bearings are considered as internal forces applied over two nodes representing the geometrical centers of the bearing.

With this approach, the system of differential equations becomes

$$([M] + [k_d] + [M_u(\dot{\theta})])\ddot{q} + ([c] + [G_d(\dot{\theta})])\dot{q} + ([k])q = F^{coup} - F^{ext} + F^{bear} \tag{13}$$

where F^{coup} represents a vector assembled with the coupling forces due to the gyroscopic effect and F^{ext} is the external effort.F^{bear} is the vector from the bearing internal forces
The main input parameters of the mechanical system represented by 13 are the vector of external forces F^{ext} in which the torque applied over the shaft causing the system to turn is included. As it was already mentioned, the bearing connecting forces F^{bear} represent the interaction between the supports and the shaft. The output is the displacement vector X.
The bearing characteristics needed for the model description are: the number of rolling ,

elements Z, the rolling element radius r, the rolling element mass m and inertia I, the inner and outer contact diameter of the rolling element with the races (Di and De), the defect frequency of the outer race BPFO , number of ranges n, contact angle of the ball and race α, ball diameter D .

The estimation of the bearing forces is based on the model of palgrem's model [23] .The nominal load on the bearing are calculated from,

$$F_n = 10.n.Z.\cos\alpha.Q_r.\frac{1}{5} \tag{14}$$

where Qr is dependent on the type of the ball bearing.In this model , we consider the ball bearing to be a rigid ball bearing and Qr is given by,

$$Q_r = \sqrt{(\frac{\delta.1000}{0.0093})^3.D} \tag{15}$$

It is to be noted that δ which is the relative displacement of the races of the bearing.we use this equation to estimate the bearing load as a function of the displacements.
The nominal torque is also calculated from the bearing forces are given by,

$$T_f = \frac{1}{2}.\mu.Di.Fn \tag{16}$$

where μ is the rolling resistance coefficient.
Finally, the load and torque variations in the bearing due its geometry i.e the BPFO is introduced in the model by,

$$\Delta F_r = a_f.\sin(BPFO.\theta).F_r \tag{17}$$

$$\Delta T_f = a_{cf}.\sin(BPFO.\theta).T_f \tag{18}$$

5.3 Results

The model was run with an external torque of 260 Nm. The value chosen for the rolling resistance coefficient was made equal to the constant friction coefficient for rigid ball bearings which is 0.0015. All other parameters are kept similar to the previous cases. The simulations are run in non stationary conditions (speed ramp up). The rotational speed is increased from 20 rad s^{-1} to 866 rad s^{-1}. The graph in figure below shows the Frequency Response in both direction for the simulations.(Figure 10)

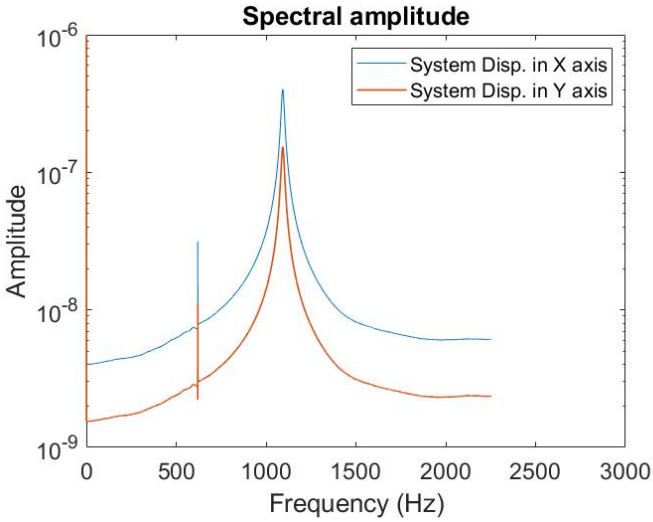

Figure 10: Frequency plot

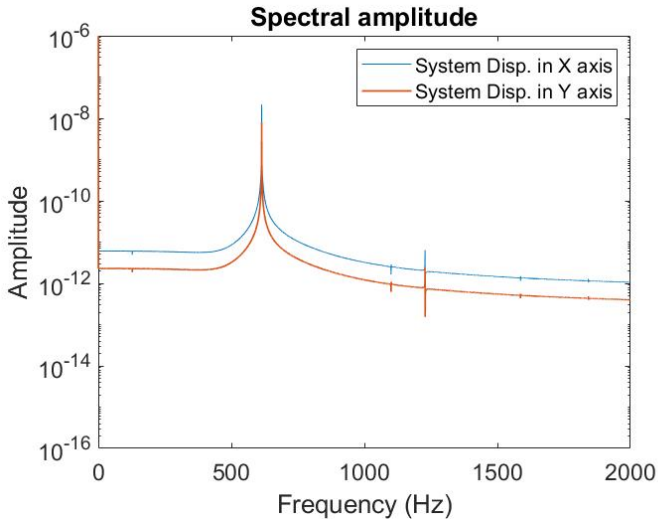

Figure 11: Frequency plot without eigen modes

(Figure 10) shows there is peak frequencies for displacements of the system in X and Y directions is associated to the load and torque fluctuation introduced by the BPFO of the ball bearing. The peak at 1100 hz shows the eigen mode and peak at 650Hz is associated to the load and torque fluctuation introduced by the BPFO of the ball bearing.
(Figure 11) shows the FRF plot for the system after removing the eigen found to focus on just the peaks due to bearing BPFO fluctuation.It shows peak at 650Hz and second harmonic at 1300Hz.

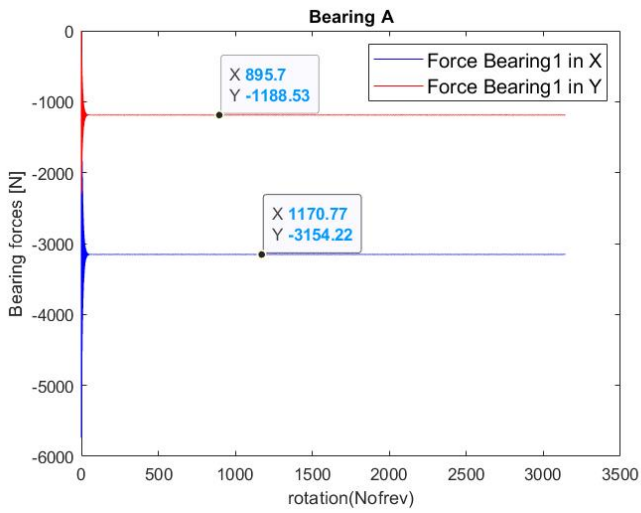

Figure 12: Bearing A Force plot

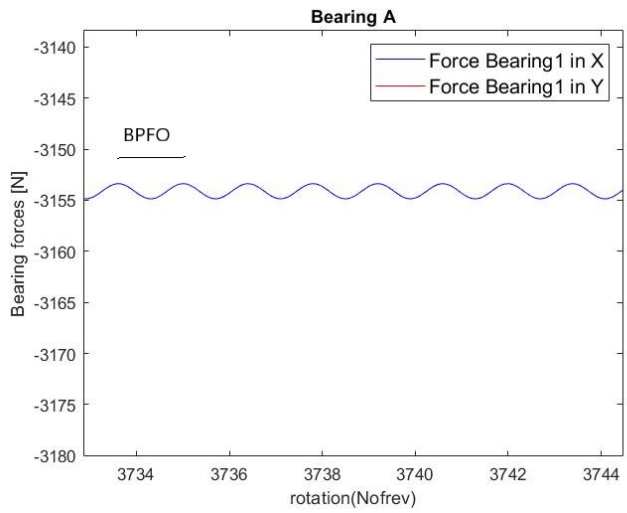

Figure 13: Zoomed View

(Figure 12) shows force plots of bearing A of the system in X and Y directions. The zoomed view in (Figure 13) shows the force fluctuation introduced by the BPFO of the ball bearing.

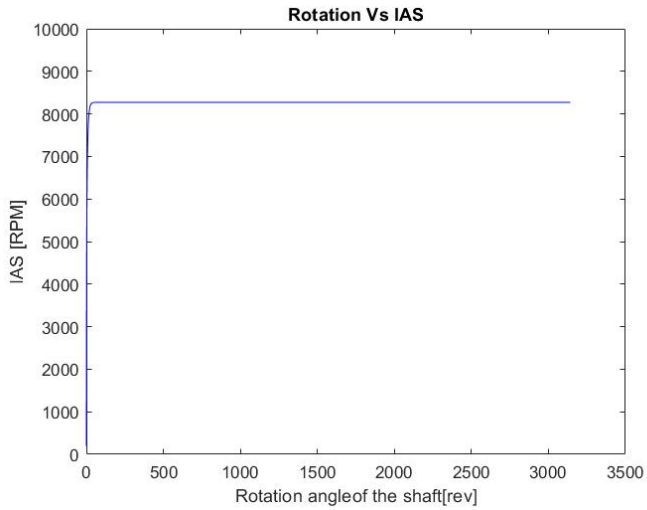

Figure 14: IAS of the Shaft

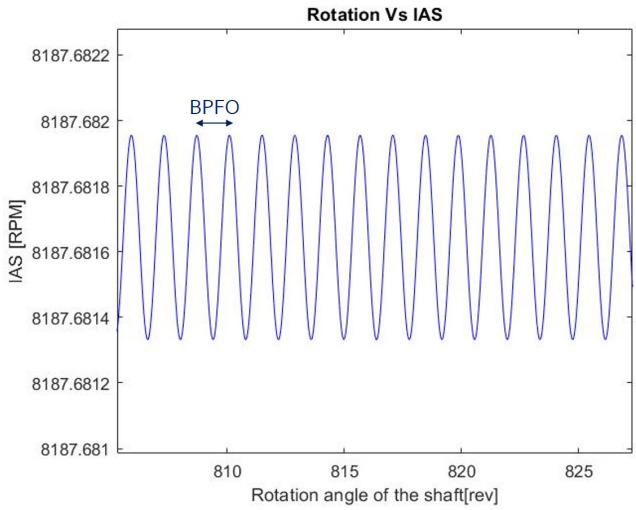

Figure 15: Zoomed View

(Figure 14) shows the response of the "macroscopic" angular speed of the system. The zoomed view in (Figure 15) shows the angular frequency of the IAS perturbation is the BPFO expressed in the angular domain which is 3.07 events per revolution. As it can be observed, the bearing oscillation has also a frequency equals to the BPFO. This phenomena is related to the evolution of the normal force distribution between the rolling elements.This simple demonstration shows us that this model is able to accurately predict the behavior of the system with coupling elements with no assumption on speed with ability to simulate the model of each element in particular for non linear and very specific behaviour.

6 Conclusion

In the first part of this report, an introduction was presented on the electric drivetrain and literature related to modeling of electric drive with a global integrated approach was reviewed and found to be very less and with a great potential to deepen the understanding of the experimental analysis. Angular Modelling technique was introduced with the emphasis on why angle domain modeling is more useful compared to classical time domain modelling in detecting cyclic perturbation. A simple academic system, in the form of Jefcott rotor is introduced to demonstrate the integration of different elements in the drive line under the assumptions that rotating speed is not constant operated under non stationary conditions. It has been observed that using Euler angle transformation to build the models, we have small difference in the peak amplitude X and Y direction when gyroscopic effects are introduced into the system. And also, splitting of the 1st and 2nd mode in eigen frequencies, and this effect is more prominent as we increase the rotational speed / decrease the rotational damping of the system when gyroscopic effects are introduced. This will be further studied when complex mechanical architectures are introduced.Next step, this modeling approach was extended to describe how the roller bearing dynamics leads to load and torque fluctuation and leads angular speed variations of the shaft.

A Apendix Numerical Simulation data

We consider a rotor made of a rigid shaft, a rigid disk and symmetric bearings. The mass unbalance is defined by Mu = 1 percent of Mass of disk and its eccentricity is given by e = 0.1 m. The damping and stiffness of the bearings are given by: cx = cy = 100 $\mathrm{N\,m^{-1}\,s}$ and kx = ky = 5×10^7 $\mathrm{N\,m^{-1}}$. The geometric and material properties of the rotor are reported in the table below:

Table 1: Properties of the system.

Symbol	Quantity	Value
L	Length of shaft	0.6 m
k1	Spring stiffness in X axis	5e7 $\mathrm{N\,m^{-1}}$
k2	Spring stiffness in Y axis	5e7 $\mathrm{N\,m^{-1}}$
f1	Radial load in X axis	50 N
f2	Radial load in Y axis	50 N
T	Torque External	300 N m
w0	initial angular velocity	20 $\mathrm{rad\,s^{-1}}$
c1	Damping in X axis	100 $\mathrm{N\,m^{-1}\,s}$
c2	Damping in Y axis	100 $\mathrm{N\,m^{-1}\,s}$
C	Damping rotational	1 $\mathrm{N\,m^{-1}\,s}$
Do	Outer shaft diameters	0.410 m
Di	Internal shaft diameter	0.079 m
ρ	Density Shaft	7870 $\mathrm{kg/m^2}$
v	Poisson Ratio	0.3
h	Thickness of disk	0.03 m

References

[1] G. Darroch. (2017) Netherlands 'will pay the price' for blocking turkish visit – erdoğan. [Online]. Available: http://newsroom.unfccc.int/media/521376/paris-electro-mobility-declaration.pd

[2] F. L. M. dos Santos, J. Anthonis, F. Naclerio, J. J. C. Gyselinck, H. Van der Auweraer, and L. C. S. Góes, "Multiphysics nvh modeling: Simulation of a switched reluctance motor for an electric vehicle," *IEEE Transactions on Industrial Electronics*, vol. 61, no. 1, pp. 469–476, 2014.

[3] C. Martis, D. Fodorean, P. C. Irimia, and C. I. Husar, "Vibroacoustic behaviour analysis of a permanent magnet synchronous machine for automotive applications," in *2014 49th International Universities Power Engineering Conference (UPEC)*, 2014, pp. 1–6.

[4] C. Guangming and X. Yudong, "A statistical model for gears noise prediction in gearbox," in *2010 International Conference on Electrical and Control Engineering*, 2010, pp. 270–272.

[5] M. Åkerblom, "Gearbox noise : Correlation with transmission error and influence of bearing preload," 2008.

[6] D. Kumar, T. Sambharam, S. Kottalgi, P. Mandloi, and O. Kesarkar, "Electric vehicle powertrain multiphysics nvh simulation," in *IECON 2018 - 44th Annual Conference of the IEEE Industrial Electronics Society*, 2018, pp. 490–495.

[7] D. Kumar, S. Kottalgi, T. Sambharam, and P. Mandloi, "A multiphysics optimization approach to design low noise and light weight electric powertrain noise, vibration and harshness (nvh) prediction of electric powertrain using finite element analysis (fea) and optimization," in *IECON 2017 - 43rd Annual Conference of the IEEE Industrial Electronics Society*, 2017, pp. 1692–1697.

[8] Y. Fang and T. Zhang, "Modeling and analysis of electric powertrain NVH under multi-source dynamic excitation," in *SAE Technical Paper Series*. SAE International, Oct. 2014. [Online]. Available: https://doi.org/10.4271/2014-01-2870

[9] N. BAYDAR and A. BALL, "Detection of gear deterioration under varying load conditions by using the instantaneous power spectrum," *Mechanical Systems and Signal Processing*, vol. 14, no. 6, pp. 907–921, 2000. [Online]. Available: https://www.sciencedirect.com/science/article/pii/S0888327099912815

[10] Z. Li, X. Yan, C. Yuan, and Z. Peng, "Intelligent fault diagnosis method for marine diesel engines using instantaneous angular speed," *Journal of Mechanical Science and Technology*, vol. 26, no. 8, pp. 2413–2423, aug 2012. [Online]. Available: https://doi.org/10.1007%2Fs12206-012-0621-2

[11] A. Yousef, F. Gu, B. Payne, and A. Ball, "Instantaneous angular speed monitoring of electric motors," *Journal of Quality in Maintenance Engineering*, vol. 10, pp. 123–135, 06 2004.

[12] S. Baudin, D. Rémond, J. Antoni, and O. Sauvage, "Non-intrusive rattle noise detection in non-stationary conditions by an angle/time cyclostationary approach," *Journal of Sound and Vibration*, vol. 366, pp. 501–513, 2016.

[13] N. Kushwaha and V. Patel, "Modelling and analysis of a cracked rotor: a review of the literature and its implications," *Archive of Applied Mechanics*, vol. 90, 06 2020.

[14] A. Bourdon, H. Andre, and D. Rémond, "Introducing angularly periodic disturbances in dynamic models of rotating systems under non-stationary conditions," *Mechanical Systems and Signal Processing*, vol. 44, no. 1-2, pp. 60–71, Feb. 2014. [Online]. Available: https://hal.archives-ouvertes.fr/hal-00916259

[15] E. Sghaier, A. Bourdon, D. Rémond, J.-L. Dion, and N. Peyret, "Coupled bending torsional vibrations of non-ideal energy source rotors under non-stationary operating conditions," *International Journal of Mechanical Sciences*, vol. 163, p. 105155, 2019. [Online]. Available: https://www.sciencedirect.com/science/article/pii/S0020740319308999

[16] S. Harsha, "Nonlinear dynamic analysis of a high-speed rotor supported by rolling element bearings," *Journal of Sound and Vibration*, vol. 290, no. 1, pp. 65–100, 2006. [Online]. Available: https://www.sciencedirect.com/science/article/pii/S0022460X05002233

[17] H. D. Nelson, "A Finite Rotating Shaft Element Using Timoshenko Beam Theory," *Journal of Mechanical Design*, vol. 102, no. 4, pp. 793–803, 10 1980. [Online]. Available: https://doi.org/10.1115/1.3254824

[18] B. Al-Bedoor, "Modeling the coupled torsional and lateral vibrations of unbalanced rotors," *Computer Methods in Applied Mechanics and Engineering*, vol. 190, no. 45, pp. 5999–6008, 2001. [Online]. Available: https://www.sciencedirect.com/science/article/pii/S0045782501002092

[19] O. Bernasconi, "Bisynchronous Torsional Vibrations in Rotating Shafts," *Journal of Applied Mechanics*, vol. 54, no. 4, pp. 893–897, 12 1987. [Online]. Available: https://doi.org/10.1115/1.3173135

[20] S. Harsha, "Nonlinear dynamic analysis of a high-speed rotor supported by rolling element bearings," *Journal of Sound and Vibration*, vol. 290, no. 1, pp. 65–100, 2006. [Online]. Available: https://www.sciencedirect.com/science/article/pii/S0022460X05002233

[21] P. McFadden and J. Smith, "Model for the vibration produced by a single point defect in a rolling element bearing," *Journal of Sound and Vibration*, vol. 96, no. 1, pp. 69–82, 1984. [Online]. Available: https://www.sciencedirect.com/science/article/pii/0022460X84905959

[22] H. HERTZ, "Uber die ber uhrung fester elastischer k orper (sur le contact entre corps elastiques)," in *J. f ur reine und angewandte Mathematik*, 1881, ch. 92, p. 156–171.

[23] P. Arvid, in *LES ROULEMENTS - Description - Théorie - Applications*, 1967, pp. 50–60.

EUROPEAN COMMISSION
RESEARCH EXECUTIVE AGENCY

“ECO DRIVE”

Noise and vibration in eco-efficient powertrains

H2020 FRAMEWORK PROGRAMME

Marie Skłodowska Curie European Training Network (ETN)

Grant Agreement 858018

Analysis of gear and bearing contact forces and strains

Deliverable no.	
Dissemination level	
Work Package	WP4
Author(s)	Lorenzo Mazzanti (ESR 11), Julian Staiger (ESR2)
Co-author(s)	Mathijs Vivet (SISW)
Status (F: final, D: draft)	F
File Name	
Project Start Date and Duration	March 1st, 2020 – February 29, 2024

Contents

1 Introduction **3**

2 The Kalman filter and Smart Virtual Sensing **3**

2.1 The discrete-time Kalman Filter 3

2.2 Multifrequency range Sensor Fusion approach 5

2.3 Smart Virtual Sensing for Contact Problems 7

3 Extension of Smart Virtual Sensing to drivetrain systems **9**

3.1 Smart Virtual Sensing for drivetrains 10

3.2 Multifrequency range Sensor Fusion for drivetrain applications 11

3.3 Constraint enforcement in Kalman filters 11

4 References **12**

1 Introduction

In recent decades, the complexity of powertrains has increased significantly as many technological developments have focused on improving both energy efficiency as well as the dynamic performance. In the automotive industry, significant efforts are currently devoted to the research and development of lightweight gearboxes to improve energy efficiency [1], while at the same time ensuring that driver and passenger comfort in terms of noise and vibrations does not deteriorate. Also, in the renewable energy sector, wind turbines are becoming ever larger to maximise energy yield [2], and this implies higher loads on the gearboxes installed in the turbines, making drivetrains an even more critical subsystem for green energy production. Also, in the renewable energy sector, wind turbines are becoming ever larger to maximise energy yield [2]. Consequently, wind turbine gearboxes are subjected to increased loads, making them even more critical subsystems for green energy production.

Within this industrial context, proper design of drivetrains and their subcomponents, such as gears and bearing, has a crucial role in ensuring efficiency and timely maintenance of components to avoid irreparable damage of the system. Monitoring the behaviour of these systems during operative conditions is fundamental to guarantee reliability and performance.

To properly address these issues, it is of paramount importance to obtain an accurate estimate of contact forces and strains acting on gears and bearings during operating conditions, so that the overall performance of the system can be evaluated [3]. However, accurate and cost-effective estimation of these quantities is rarely possible with experimental methods, as obtaining direct measurements is difficult and labour intensive. Estimates are only approximately available using numerical methods, such as forward Finite Element or flexible multibody simulation. This forces engineers to oversize their designs, thus losing potential efficiency gains that could be obtained with a more thorough knowledge of the system's behavior. A more accurate estimate of the system's state could also be used by maintenance engineers to develop a better understanding of the critical gear and bearing contact loads and the resulting component stresses that lead to accumulated damage over the course of the drivetrain's deployment.

In recent years, significant efforts have been spent on developing hybrid deterministic-stochastic techniques, which enhance the predictive performance of numerical models with real-world measured data. The *Smart Virtual Sensing* (SVS) framework, which uses the Kalman filter estimator as one of its algorithmic building blocks to combine measurement data with numerical models, is finding more and more traction in the field of structural dynamics, where it has found application in various industrially relevant cases [4]–[7].

This technical report explores how this innovative framework can be used for the task of contact force and strain estimation during operative conditions of drivetrain systems, while highlighting the technical challenges to be solved for proper implementation and discussing some of the current limitations the SVS approach has for this type of applications.

2 The Kalman filter and Smart Virtual Sensing

This section gives an insight into the estimator used in the SVS framework and its applications. The discrete-time formulation of the Kalman Filter (KF) is presented in Section 2.1. The idea of an application in the multi-frequency domain and thus an extension of the SVS framework to a wider frequency range is presented in Section 2.2. Furthermore, an example application of the SVS framework to a contact problem is shown in Section 2.3.

2.1 The discrete-time Kalman Filter

In this section, the for the SVS framework used state estimator algorithm namely the Kalman Filter is explained. For the sake of this report, we assume a linear and time-invariant system and therefore a linear discrete-time Kalman filter is chosen for state estimation [8]. The algorithm can also be exploited for nonlinear problems as has been shown in [9].

The Kalman filter is a stochastic-deterministic approach that combines a process model and a number of measurements. Statistical noise, which is assumed to be of Gaussian nature is taken into account on both the process $\boldsymbol{w}_i = \mathcal{N}(0, \boldsymbol{Q})$ and the measurements $\boldsymbol{v}_i = \mathcal{N}(0, \boldsymbol{R})$. In previous scientific works, it has been shown that a Kalman filter can be successfully used to estimate the system states more accurately than using only time integration or a simple forward simulation [10], [11]. This enables the filter to function as a virtual sensor and allows the user to estimate states in locations where physical measurements are not feasible due to the e.g. intrusive nature of sensors used or the inaccessibility. The process of Kalman filtering is also referred to by some authors as sensor fusion because it also allows combining different measurements of the same quantity as long as the noise characteristics of the respective sensors are determined.

The algorithm is twofold. First a prediction is computed based on the model, this is followed by an update step during which the state is corrected using the measurement data. The latter step is often also referred to as the innovation.

Prediction:

$$\hat{\boldsymbol{x}}_k^- = \boldsymbol{A}\hat{\boldsymbol{x}}_{k-1}^+ \tag{1}$$

$$\boldsymbol{P}_k^- = \boldsymbol{A}\boldsymbol{P}_k^-\boldsymbol{A}^{\boldsymbol{T}} + \boldsymbol{Q} \tag{2}$$

Correction:

$$\boldsymbol{K}_k = \boldsymbol{P}_k^-\boldsymbol{H}^T(\boldsymbol{H}\boldsymbol{P}_k^-\boldsymbol{H}^T + \boldsymbol{R})^{-1} \tag{3}$$

$$\hat{\boldsymbol{x}}_k^+ = \hat{\boldsymbol{x}}_k^- + \boldsymbol{K}_k(\boldsymbol{y} - \boldsymbol{H}\hat{\boldsymbol{x}}_k^+) \tag{4}$$

$$\boldsymbol{P}_k^+ = (\boldsymbol{I} - \boldsymbol{K}_k\boldsymbol{H})\boldsymbol{P}_k^-. \tag{5}$$

Where $\hat{\boldsymbol{x}}_k$ is the discrete state vector at timestep k, $\boldsymbol{A}$ is the discrete state transition matrix, $\boldsymbol{P}$ is the error covariance, $\boldsymbol{K}$ is the Kalman gain, $\boldsymbol{y}$ the vector of real measurements and $\boldsymbol{H}$ the measurement matrix.

In order to construct a stable observer, meaning to prevent the divergence of states, the underlying system must be observable. One of the most popular observability metrics for Kalman filter based estimators is the observability matrix rank criterion. It was proposed by Kalman himself and considers a system to be observable if the observability matrix $\boldsymbol{O}_k = [\boldsymbol{H} \quad \boldsymbol{HA} \quad \dots \quad \boldsymbol{HA}^{n-1}]^T$ has full column rank. Recently also the condition number of $\boldsymbol{O}_k$ has been considered for the evaluation of observability [7]. When the condition number is large the matrix $\boldsymbol{O}_k$ is poorly conditioned and this indicates a rank deficiency.

The prior introduced matrix rank criterion let one sharply distinguish between a not observable and an observable system. By using the condition number, one can compare different sensor layouts for the same test setup, which all result in a formally observable system by means of the matrix rank criterion. Since one can expect that the estimation of a system states will only improve by adding new sensor information to an already observable system, this means that in practice one can use the condition number to identify how much additional information a sensor in a certain location adds to the observability of a system.

2.2 Multifrequency range Sensor Fusion approach

One general assumption in Kalman filtering is that the involved sensors are used in their characteristic bandwidth only. For this assumption, the measurement matrix $\boldsymbol{H}$ is constant over the whole frequency range.

$$\boldsymbol{H}(\boldsymbol{s}) = \boldsymbol{const.}\ \forall\, \boldsymbol{s} \in \mathbb{C}. \tag{6}$$

Plenty of research has been carried out investigating the proper placement of sensors to achieve high observability [7], [12]. However, different sensors show a variety of bandwidth characteristics which are, amongst other information, usually given in the sensor datasheet, Figure 1.

NOISE PERFORMANCE					
Rate Noise Density	T_A = 25°C		0.04		°/sec/√Hz
FREQUENCY RESPONSE					
Bandwidth[4]		1		1000	Hz
Sensor Resonant Frequency			14.5		kHz
SELF-TEST (RATIOMETRIC)[1]					
ST1 Rate-Out Response	ST1 pin from Logic 0 to Logic 1		−1.9		V
ST2 Rate-Out Response	ST2 pin from Logic 0 to Logic 1		1.9		V
Logic 1 Input Voltage		$0.8 \times V_{RATIO}$			V
Logic 0 Input Voltage				$0.2 \times V_{RATIO}$	V
Input Impedance	To common		50		kΩ

Figure 1: excerpt of sensor datasheet ADXRS624.

Thus, the selection of the sensors must therefore be made according to the frequency range in which one suspects the variables to be observed. Usually, the practitioner is choosing only sensors covering the whole bandwidth in which the states of interest are expected to ensure a proper prediction of all significant states.

However, sensors that can accurately measure over a larger bandwidth, are usually more expensive when compared to those that have a narrower measuring bandwidth. Therefore, the sensor instrumentation in terms of bandwidth is often oversized. For the sake of comparison, Table 1 lists two MEMS accelerometers with different bandwidths and their costs while all other sensor characteristics remain identical.

Table 1: comparison of two accelerometers.

Part number	# of axes	Range (g)	Bandwidth (Hz)	Price ($)
ADXL1005	1	100	1-23k	40.00
ADXL1001	1	100	1-11k	30.00

Furthermore, sensor fusion often means fusing data from multiple sensors of the same make, all covering the full bandwidth of the system as described above. However, sensor fusion between different sensor types might also not be feasible due to a lack of shared bandwidth. A possible example would be the combination of MEMS accelerometers, piezo accelerometers and MEMS gyroscopes which all show a distinctive behaviour in the frequency domain.

As discussed in Section 2.1 adding more sensor information can be beneficial even in cases when the system is already formally observable. Adding different sensor information e.g. acceleration, velocity and position to the measurement matrix $\boldsymbol{H}$ decreases the condition number of $\boldsymbol{O}_k$. However, finding a suitable frequency band for all sensors, which corresponds to the frequency band in which the states are estimated, is not a trivial task. The latter becomes even more challenging when different types of measurements must be considered.

The combination of sensors with different bandwidths inevitably leads to a violation of Eq. (**6**) and therefore introduces systematic errors in the state estimation. This is the main reason why the behaviour of the system model, used in the KF, may not match that of the real-world system [13]. A block diagram of the estimation chain is given in Figure 2. As soon as the *Sensors* block introduces a certain amount of dynamics and hence $\tilde{\boldsymbol{y}}(t) \neq \boldsymbol{y}(t)$, the system model used in the Kalman filter does not represent the real system anymore. The estimation of the system states $\hat{\boldsymbol{x}}(t)$ and the inputs $\hat{u}(t)$ is hence biased.

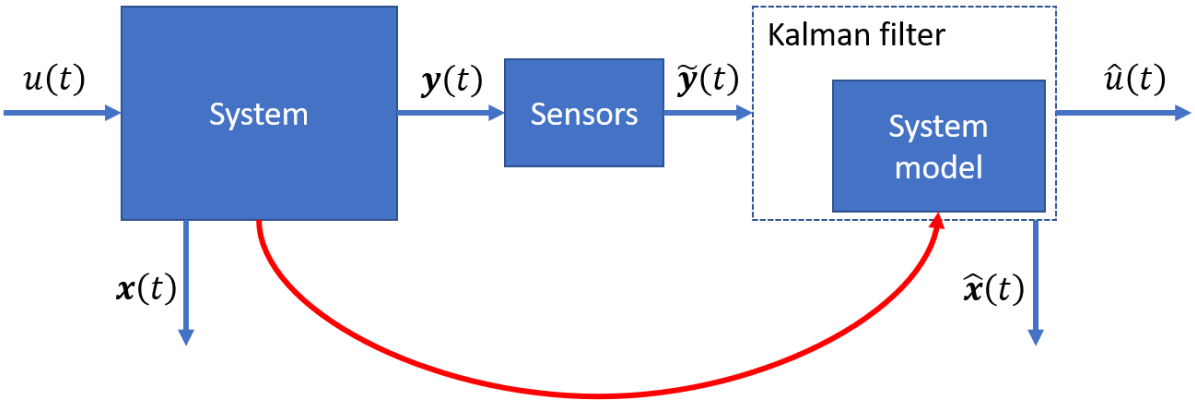

Figure 2: estimation chain normal approach.

The proposed approach is to include sensor dynamics into the process model used in the Kalman filter itself. It can be therefore considered a Multifrequency range Sensor Fusion (MSF) approach taking the frequency characteristics of sensors into account. A schematic overview is presented in Figure 3. The MSF allows using sensors with frequency characteristics that do not coincide or even lay far apart from each other. It offers the possibility to combine multiple sensors from different manufacturers and with different frequency characteristics as well as the combination of sensors not combined before in the field of structural estimation e.g. accelerometers and gyroscopes.

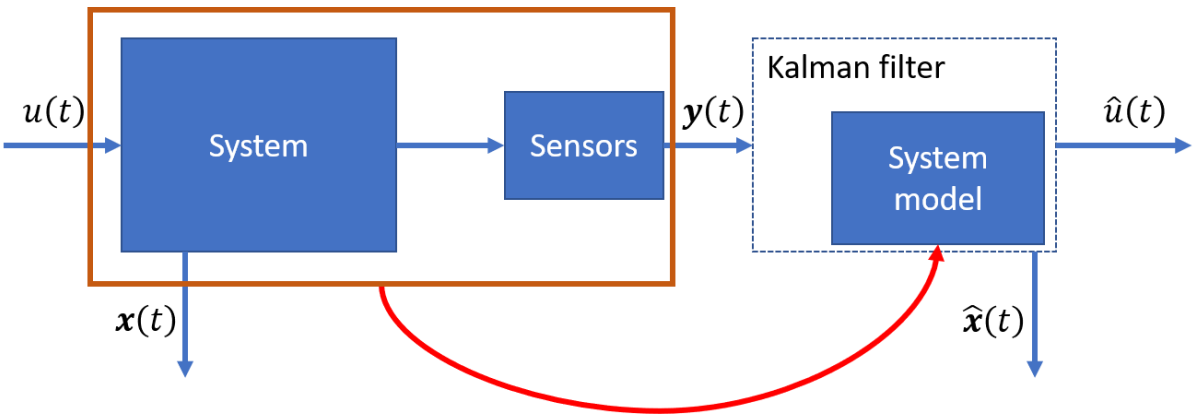

Figure 3: estimation chain MSF approach.

As sensors are mechatronic systems and extensive research on their operation and design is published one can combine any physical system model with the equivalent sensor representation to one summarised system model. The size of the system model used in the Kalman filter is increasing which affects the computational load in the algorithm. However, most sensor behaviour can be expressed with three additional states which sufficiently captures the bandpass characteristic of the sensor. Since the number of states is usually higher than the number of sensors involved, the contribution of the increase in states through the application of the MSF approach is small compared to other factors that would increase the accuracy of the estimation, e.g. a finer discretization of the system.

2.3 Smart Virtual Sensing for Contact Problems

Simulation of drivetrain systems requires the solution of contact problems to properly model the interactions between transmission subcomponents (e.g., teeth contact between gears). The presence of contact phenomena implies deviations from the linear, time-invariant assumptions made in the Section 2.1 definition for the KF. Several KF formulations for nonlinear applications have already been developed and have been adopted within different fields and across a wide variety of industrial applications [9], [14]. In this subsection, a simplified, virtual contact mechanics case is presented as an example to describe how the SVS framework can be used to update relevant model parameter to obtain more accurate estimations even when dealing with the non-smoothness associated with contact mechanics.

As a starting point, consider two gears meshing (Figure 4, top). Gear contact is a difficult problem to simulate, with many researchers active in the field [15]. The definition of an SVS framework for this type of application poses significant challenges in terms of proper implementation. Therefore, in the context of this report, the problem is simplified via a representative lumped parameters model of an equivalent mass-spring-damper (MSD) system, which is shown in Figure 4 (bottom). Four spherical bodies are connected via spring-damper elements. Each pair of bodies is used to represent one of the gear's body and gear tooth in contact (bodies 1-2 for gear on the left, bodies 3-4 for the gear on the right).

Body 1 is put into periodic motion by an actuator. As a result, body 2 and 3 come into contact multiple times during the simulation. To represent the contact interaction between teeth, a Hertzian contact force element [16] is defined between body 2 and 3.

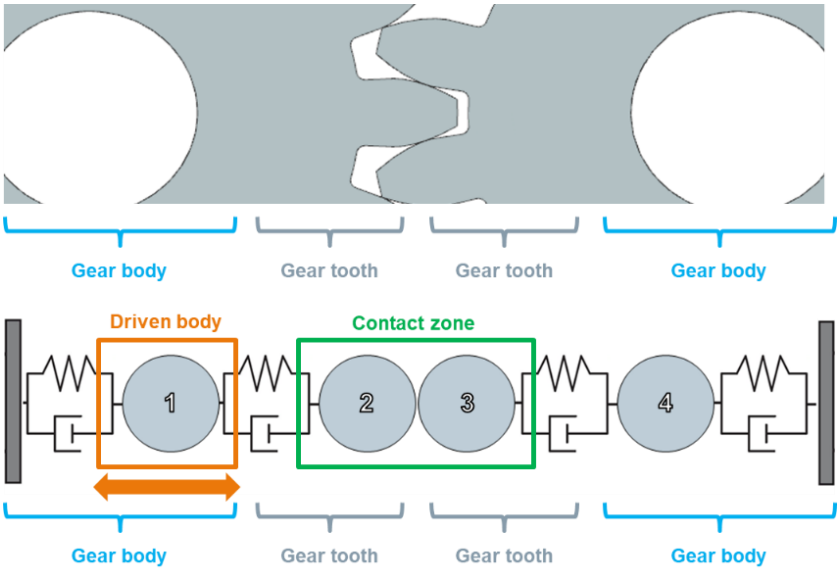

Figure 4: systems considered in the virtual experiment.

The contact force element computes a contact reaction force F_c, according to the equation:

$$F_c = K(\text{bodies' geometry and material})\ \delta^{\frac{3}{2}} \tag{7}$$

In Eq. (7) the value of contact stiffness parameter K is dependent on the geometry and the material properties of the bodies in contact, while the amount of relative penetration δ between these bodies is computed under the assumption of a rigid contacting surfaces.

In the context of this virtual example and to showcase how SVS can be adapted to contact mechanics applications, the parameter K is inserted in the SVS framework, following the workflow in Figure 5.

Two models are considered:

1. An accurate MSD model, which represents the real-world reference, is used to obtain the measurement signals.
2. An inaccurate MSD model, which represents the approximative model that is available to the simulation engineer and thus contains some uncertainties or inaccuracies for one or more model parameters. In this case, the contact stiffness K is different from the reference.

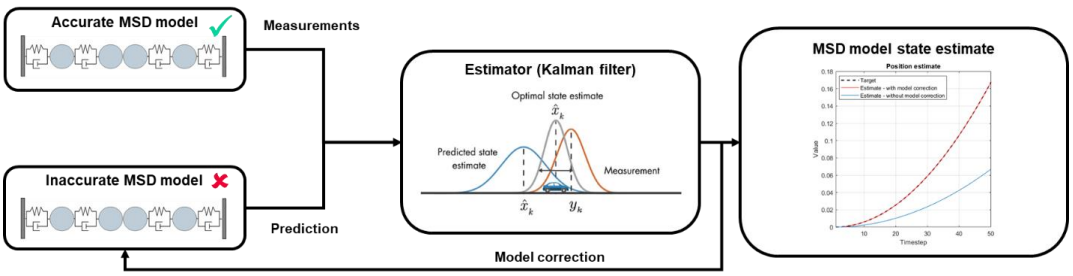

Figure 5: SVS workflow for the virtual experiment.

The estimator takes as input (1) the measurement signals computed by the reference model and (2) the state prediction provided by the inaccurate model. Both are combined to produce a corrected state estimate and a value correction on the user-defined parameters to update the inaccurate model based on the measured signal.

The contact stiffness parameter K was chosen as the target for the above parameter estimation example since it is one of the most difficult aspects to accurately represent within a contact model. Consequently, it is also reasonable to assume that here the most uncertainty is introduced into the model. Detecting and correcting inaccuracies in the contact model parameters is therefore hugely beneficial for improving the accuracy of the overall estimation.

Some considerations have to be made in terms of estimator stability for this application. As explained in Section 2.1, observability of the estimated parameters is important for the sake the estimation process' accuracy. Given the nature of the contact problem and with reference to the example of Figure 4, it's possible to verify that the parameter K is observable only when contact between bodies 2-3 is occurring. The same conclusion could be reached from physical intuition, as the contact stiffness parameter K only influences the system whenever the contact interaction is active.

Following the representation of the gear meshing problem by the MSD system, presented in Fig. 4, the gear tooth strains for each gear are simplified in the MSD model, using the relative displacements between bodies 1-2 and 3-4. The objective of the estimation process can therefore be easily extended to the accurate estimation of these signals.

The parameter estimation result is presented in Figure 6. The black line is the correct target value, the blue curve shows the incorrect parameter value that is obtained by the inaccurate MSD model, and the red curve is the evolution of the parameter estimate throughout the estimation process. After an initial oscillation, the estimated stiffness converges to the target.

Figure 7 shows the effect that the parameter correction has on the predicted strain level. The black curve is the target strain value, while the dotted blue is the strain signal obtained by the inaccurate MSD model, and the dotted red is the strain estimate computed using the SVS framework to correct the stiffness parameter K. As a result of the contact model parameter update, the strain signals are more accurately estimated.

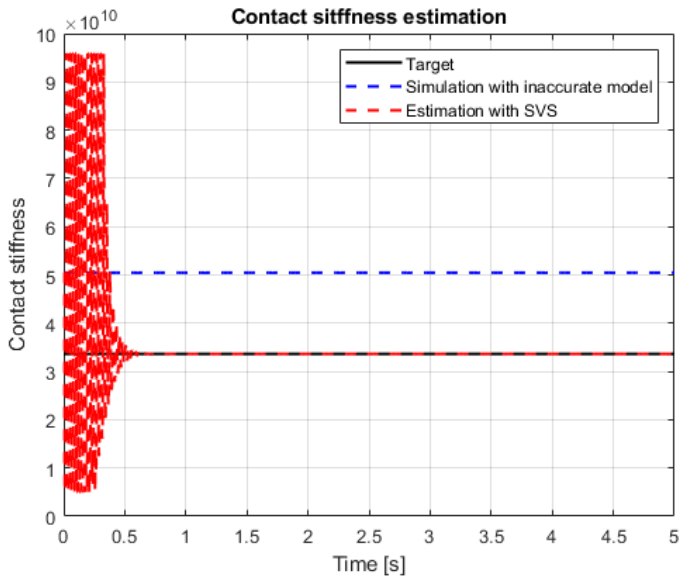

Figure 6: contact stiffness estimation results.

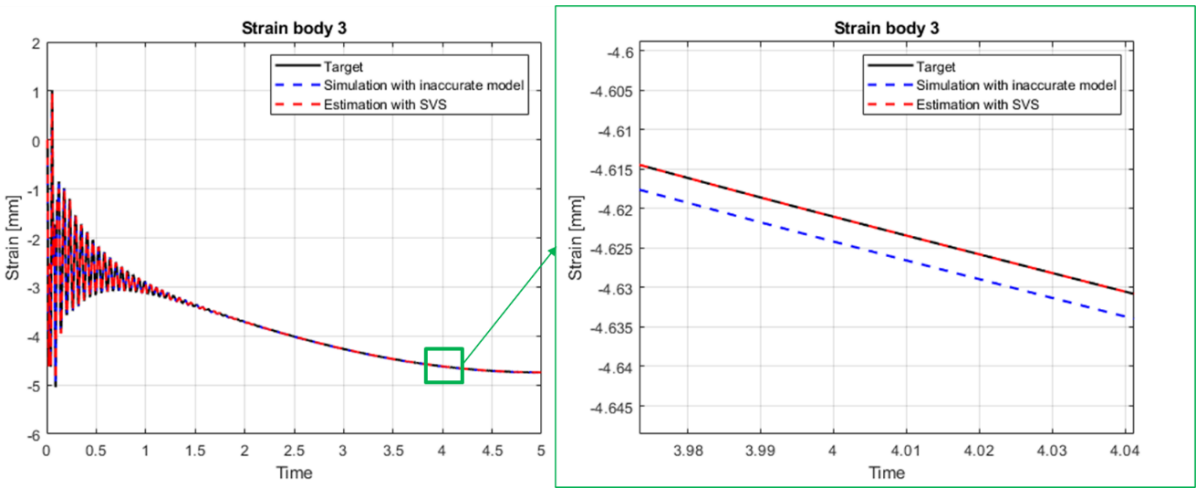

Figure 7: strain estimation results for body 3.

3 Extension of Smart Virtual Sensing to drivetrain systems

The main objective of the task is the extension of the SVS framework to drivetrain applications, focusing on prediction of contact forces and strains under operative conditions. Detailed numerical models that are used to simulate gear and bearing dynamic behaviour, will be combined with the already developed SVS framework in order to perform accurate parameter estimation, while using real-world data as a reference. A graphical representation of the SVS framework workflow for drivetrain application is visible in Figure 8.

A flexible multibody simulation environment, for which recently several state-of-the-art simulation solutions for drivetrain components have been developed [3], [15], is selected as the mathematical framework to further develop the presented SVS approach. To reach the objective of accurate contact forces and strain estimation, several technical challenges must be addressed.

Section 3.1 introduces the concept of SVS for drivetrains; Section 3.2 presents possibilities for further use of the MSF approach for drivetrain applications; Section 3.3 is dedicated to the discussion of constraints enforcement during the estimation process.

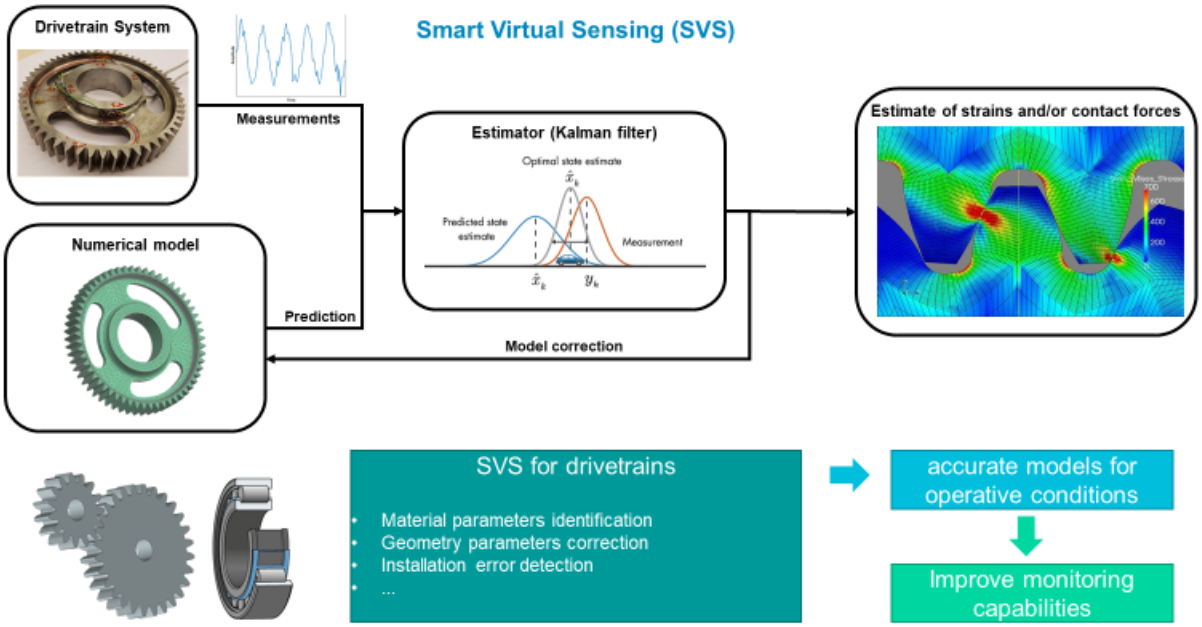

Figure 8: an overview of the SVS framework for drivetrains.

3.1 Smart Virtual Sensing for drivetrains

The principle at the heart of SVS is the concept of updating model parameters to match real-world data. Given the target that it is desirable to reach, i.e., the estimation of contact forces in gears and bearings under operative conditions, it is of the utmost importance to determine which set of model parameters must be included in the SVS update loop to obtain an accurate estimation.

The ideal models to target for this application are the ones directly related to the simulation of gears and bearings contacts. These models use many parameters, and significant time will be spent on researching which parameter set is more apt for the task of estimating contact forces and strains.

Estimation of material parameters, such as density or Young modulus, could prove greatly beneficial for improving model accuracy, as they are fundamental parameters that affect the overall physical behaviour of the considered drivetrain components.

Correction of geometrical parameters could also improve estimation capabilities, as gear and bearing models require the definition of highly detailed geometry parameters sets, whose knowledge may not even be complete and based on prior assumptions.

Another important application of the SVS framework could be in the field of installation error detection. When building a multibody model of a drivetrain, the user often assumes that gears are mounted in the correct position and angle, while in real-world applications this is not necessarily the case, misalignments often occur. This gap between models and reality could be reduced by an SVS application that is capable of estimating misalignments or centre-line offsets between gear pairs and correctly applying them to the models during the estimation process.

Pitting detection could also prove to be an important application of the SVS framework for drivetrains. With a proper parametrization of the teeth's flank of gears, the estimator could try to estimate deviations of the estimated flank from the design profile, thus helping in the identification of surface pitting.

3.2 Multifrequency range Sensor Fusion for drivetrain applications

The MSF approach aims to combine system with sensor models that can be used together in an estimator to account for the dynamic effects introduced by the sensors. This approach will allow the number of high accuracy/high bandwidth sensors to be reduced and replaced with lower-cost alternatives or enhance the overall performance of estimators at the boundaries of the bandwidth of the sensors involved. In addition, it is also possible to combine sensors that are not normally combined in Kalman filters due to mismatching bandwidths, such as accelerometers and microphones.

Concerning the application of the MSF concept in powertrain applications, several possibilities are conceivable. Forrier et al. [17] established an estimator for broadband torque estimation in powertrains. They assumed the used rotational velocity and Ferraris sensors to be ideal although they show distinctive bandwidth characteristics. Incorporating the MSF approach in a similar scheme could be promising to enhance the broadband torque estimation even further.

Another way to use the MSF approach would be to replace optical rotational speed sensors with MEMS gyroscopes attached directly to the rotating parts. This would also have the advantage that the rotating parts do not have to be mechanically machined before the measuring devices can be used, as is the case with optical sensors. Thus, a larger set of potential measuring points is conceivable.

3.3 Constraint enforcement in Kalman filters

Besides the integration of the SVS framework into the FMB formulation, one of the most important ongoing methodological developments focuses on overcoming the numerical challenges that arise when model constrains must be enforced during the estimation process. As it's possible to infer from Section 0, the classical formulation of the KF does not consider any system constraint when applying corrections to state estimates and model parameters. This can produce numerical problems when applying KF to multibody problems, as the equation of motion of these systems generally comprises some constraints that arise from the presence of joints, used to limit the bodies' range of motion. This conflict between the numerical model and KF's formulations inevitably leads to instability and inaccuracy of the estimation.

Additional problems can arise when performing parameter estimation. Since the KF has no prior knowledge about the nature of the parameters to be estimated, it is possible to obtain parameter estimates whose value does not consider any physical information or limitations of the parameter. To give an example, we can consider the unconstrained parameter estimation of the inertia properties (e.g., the mass of a rigid body). Without the presence of any parameter constraints, it is theoretically possible that the outcome of the KF correction step produces an estimate of a negative mass. This does not make sense from a physical point of view and will necessarily create problems when integrating the system's equation of motion during the next timestep. To avoid this sort of problem altogether, additional inequality constraint equations should be introduced to bound the filter's corrective step within a user-imposed or physics-based range of correct updates.

The development of a constraint enforcement methodology that is specific to the problem at hand is therefore an important and necessary step in advancing the current SVS capabilities and extending the framework to the field of flexible multibody drivetrain estimation. Two classes of constraints that should be enforced during the estimation process have been identified in this section, multibody-related and parameter-related. Several solutions for linear and nonlinear constraints enforcement in KFs have been proposed in literature [9], [18], but none specifically deals with enforcing equality and inequality constraints in an SVS-multibody setting. Significant effort will be spent on developing this fundamental methodological advancement.

4 References

[1] S. Shweiki, A. Rezayat, T. Tamarozzi, and D. Mundo, “Transmission Error and strain analysis of lightweight gears by using a hybrid FE-analytical gear contact model,” *Mechanical Systems and Signal Processing*, vol. 123, 2019, doi: 10.1016/j.ymssp.2019.01.024.

[2] *MARE-WINT*. 2016. doi: 10.1007/978-3-319-39095-6.

[3] B. Blockmans, T. Tamarozzi, F. Naets, and W. Desmet, “A nonlinear parametric model reduction method for efficient gear contact simulations,” *International Journal for Numerical Methods in Engineering*, vol. 102, no. 5, 2015, doi: 10.1002/nme.4831.

[4] F. Naets, J. Cuadrado, and W. Desmet, “Stable force identification in structural dynamics using Kalman filtering and dummy-measurements,” *Mechanical Systems and Signal Processing*, vol. 50–51, 2015, doi: 10.1016/j.ymssp.2014.05.042.

[5] E. Risaliti, T. Tamarozzi, M. Vermaut, B. Cornelis, and W. Desmet, “Multibody model based estimation of multiple loads and strain field on a vehicle suspension system,” *Mechanical Systems and Signal Processing*, vol. 123, pp. 1–25, May 2019, doi: 10.1016/J.YMSSP.2018.12.024.

[6] T. Uhl, “The inverse identification problem and its technical application,” in *Archive of Applied Mechanics*, 2007, vol. 77, no. 5. doi: 10.1007/s00419-006-0086-9.

[7] R. Cumbo, L. Mazzanti, T. Tamarozzi, P. Jiranek, W. Desmet, and F. Naets, “Advanced optimal sensor placement for Kalman-based multiple-input estimation,” *Mechanical Systems and Signal Processing*, vol. 160, p. 107830, Nov. 2021, doi: 10.1016/J.YMSSP.2021.107830.

[8] R. E. Kalman, “A new approach to linear filtering and prediction problems,” *Journal of Fluids Engineering, Transactions of the ASME*, vol. 82, no. 1, 1960, doi: 10.1115/1.3662552.

[9] D. Simon, *Optimal state estimation: Kalman, H∞, and nonlinear approaches*. 2006. doi: 10.1002/0470045345.

[10] S. van Ophem, E. Deckers, and W. Desmet, “Model based virtual intensity measurements for exterior vibro-acoustic radiation,” *Mechanical Systems and Signal Processing*, vol. 134, 2019, doi: 10.1016/j.ymssp.2019.106315.

[11] E. Lourens, E. Reynders, G. de Roeck, G. Degrande, and G. Lombaert, “An augmented Kalman filter for force identification in structural dynamics,” *Mechanical Systems and Signal Processing*, vol. 27, no. 1, 2012, doi: 10.1016/j.ymssp.2011.09.025.

[12] H. Zhang, R. Ayoub, and S. Sundaram, “Sensor selection for Kalman filtering of linear dynamical systems: Complexity, limitations and greedy algorithms,” *Automatica*, vol. 78, 2017, doi: 10.1016/j.automatica.2016.12.025.

[13] J. Vilà-Valls, E. Chaumette, F. Vincent, and P. Closas, “Modelling mismatch and noise statistics uncertainty in linear MMSE estimation,” in *European Signal Processing Conference*, 2019, vol. 2019-Septe. doi: 10.23919/EUSIPCO.2019.8903118.

[14] M. N. Chatzis, E. N. Chatzi, and S. P. Triantafyllou, “A Discontinuous Extended Kalman Filter for non-smooth dynamic problems,” *Mechanical Systems and Signal Processing*, vol. 92, 2017, doi: 10.1016/j.ymssp.2017.01.021.

[15] N. Cappellini, T. Tamarozzi, B. Blockmans, J. Fiszer, F. Cosco, and W. Desmet, “Semi-analytic contact technique in a non-linear parametric model order reduction method for gear simulations,” *Meccanica*, vol. 53, no. 1–2, 2018, doi: 10.1007/s11012-017-0710-5.

[16] A. M. S. Budynas, Richard G., “Roark’s Formulas for Stress and Strain, Ninth Edition,” *Studies in Applied Mechanics*, vol. 4, no. C, 1980.

[17] B. Forrier, F. Naets, and W. Desmet, “Broadband load torque estimation in mechatronic powertrains using nonlinear kalman filtering,” *IEEE Transactions on Industrial Electronics*, vol. 65, no. 3, 2018, doi: 10.1109/TIE.2017.2739709.

[18] B. O. S. Teixeira, J. Chandrasekar, L. A. B. Tôrres, L. A. Aguirre, and D. S. Bernstein, “State estimation for linear and non-linear equality-constrained systems,” *International Journal of Control*, vol. 82, no. 5, pp. 918–936, 2009, doi: 10.1080/00207170802370033.

EUROPEAN COMMISSION
RESEARCH EXECUTIVE AGENCY

“ECO DRIVE”

Noise and vibration in eco-efficient powertrains

H2020 FRAMEWORK PROGRAMME

Marie Skłodowska Curie European Training Network (ETN)

Grant Agreement 858018

Analysis of transmission induced vibrations and noise

Deliverable no.	
Dissemination level	
Work Package	WP4
Author(s)	Khadijeh FARSHI (ESR5), Navdeep SHARMA (ESR6)
Co-author(s)	
Status (F: final, D: draft)	F
File Name	
Project Start Date and Duration	March 1st, 2020 – February 29, 2024

Table of Contents

1 Introduction **3**

2 Analysis of transmission-induced vibrations and noise **4**

2.1 Psychoacoustic analysis 4

2.2 Simulation based analysis 5

3 ECO DRIVE ESR activities **6**

3.1 ESR5 - NVH measurement and analysis methods focused on engine-transmission-unit 6

3.2 ESR6 - Sensitivity analysis of lightweight design concepts in terms of gearbox acoustics 9

1 Introduction

In the recent times, the transport sector has been subjected to increasing stringent regulatory guidelines pertaining to environmental emissions. The response of the automobile manufacturers has been to move development efforts towards creating product portfolios exploiting new technologies that reduce pollution effects. However, there are some adverse effects in the use of these new technologies, particularly in terms of the noise characters of these products.

The shift to electric vehicles (EV) eliminates the masking effect of the noise from conventional internal combustion (IC) engines, which renders secondary noise sources like road noise, wind noise and HVAC noise more prominent. There is also an addition of noise from new auxiliary systems that support hybrid/electric propulsion platforms. Albeit the overall interior and exterior noise levels of these vehicles is lower than the conventional alternatives, there are negative health effects due to relatively higher high-frequency content in EVs. Development of lightweight vehicles, in the aim of increasing efficiency and reducing fuel emissions, has its own noise management challenges as thinner and lighter structures are by vibro-acoustic principles more prone to vibration problems.

The ECO DRIVE project aims to address these issues through research on several technical-scientific topics linked to the NVH performance of the next generation of downsized IC engines, e-motors, lightweight transmission systems and drivelines.

2 Analysis of transmission-induced vibrations and noise

This document briefs the task on the analysis of transmission induced vibrations and noise from the project workpackage WP2 on lightweight transmission systems and drivelines. The complexity of the NVH challenges from highly interconnected powertrain elements requires multi-attribute testing and simulation techniques. Advancement on the task is planned through collaboration of ESRs and research activities on (i) advanced testing and analysis methods (ESR5), and on (ii) virtual and hybrid approaches (ESR6).

2.1 Psychoacoustic analysis

One of the most important topics of the automotive industry is the development of fuel-efficient vehicles. Besides achieving lightweight vehicles to reduce the fuel consumption, developing powertrains design with minimum noise and vibration level is a vital target in the automotive industry to meet the customer's comfort. By decreasing the weight of the system, the ratio of stiffness to mass in the system is increased, so the eigenfrequencies of the vehicle shift to a higher frequency range. Furthermore, with the increased rotational speeds of electrical drives, the higher frequency resonances are more likely to be excited. Additionally, in electrical vehicles (EV) NVH problems occur because of the reduced noise floor due to the absence of the masking effect of internal combustion (IC) engines which makes the auxiliary components more noticeable. Sometimes it is assumed that EV are more silent, but the fact is that in reality they produce a great number of high-frequency noise (Fischer, J., 2017).

Identifying of the sources of the emitted noises in the lightweight powertrain and characteristics of these noises is necessary to remove or decrease the more annoying noises for the drivers. It is important to note that considering only sound pressure level and overall vibration is not enough, other characteristics of noise such as sharpness, roughness, loudness, and tonality (so called psychoacoustic metrics) need to be considered. These metrics can then be used to prioritize, which of the noises are most annoying to the drivers. To do this, a correlation between the NVH measurements and human perception can be shown, by mapping the measurements to psychological factors via psychoacoustic analysis.

Developing a test-based method for the noise optimization of gearboxes by considering lightweight specification and psychoacoustic metrics would be practical and useful for achieving a comfort increase for the passengers in the vehicle cabin.

2.2 Simulation based analysis

Using suitable simulation tools, digital twins for novel gearbox configurations can be conceived and evaluated for their physical dynamics. Advances in simulation techniques, particularly in multi-body dynamics (MBD) and numerical methods (FEM/BEM) can help model relevant physical phenomena linked to the NVH behaviour of gearboxes.

Downsized drivetrains very commonly make use of light and relatively more flexible structures. These structures employ components with high elastic response which directly affects the gear-mesh excitations and the vibration transfer paths of the gearbox. For example, higher flexibilities of gear blanks, shafts and housings can cause larger tooth misalignments, which can lead to higher system excitations and a worsened acoustic performance. Simulation-based sensitivity analyses and parameter studies can help identify the risks and capabilities of these lightweight designs in terms of the gearbox's acoustic performance.

The prime excitation in a gearbox is the harmonic gear-mesh force which travels through flexible shafts and bearings and finally excites the housing structure. This excitation chain can be virtually evaluated and different metrics like transmission errors, bearing loads and housing surface velocities can be studied to rank the influence of problematic components. Targeted adaptation to these identified components can lead to new possible design concepts for gearboxes which can be then benchmarked against the best-available current systems.

Along with the investigation of lightweight construction techniques, new production technologies, can be modelled and studied. Recent development in additive manufacturing and selective laser melting can be employed to develop novel part geometries. The use of alternative materials and acoustically promising configurations (e.g., foam structures or meta-materials) can also be explored.

3 ECO DRIVE ESR activities

3.1 ESR5 - NVH measurement and analysis methods focused on engine-transmission-unit

Noise level control of gear mechanisms is not only to embody the comprehensive strength of a manufacturing enterprise but also subjected to environmental law and regulation. While there are many sources of noise in a vehicle, this project will focus on the noise that is emitted from engines and powertrains. Providing a more comfortable vehicle to passengers is always one of the main goals of vehicle development and reducing the noise and vibration of vehicles according to customers' expectations plays a vital role in this regard. The research on reducing gearbox vibration and noise began a century ago; however, vibration and noise as a major factor to evaluate performance of a mechanism began in the middle of the 1960s. In the early stage, based on much research of experiments and tests, scholars obtained an empirical formula for estimating the noise intensity of gear pairs. The appearance of numerical methods such as the finite element method (FEM) and boundary element method (BEM), has supported research on reducing vibration and noise (Maier, T., 2011). The FEM/BEM method is the prevailing method applied to numerical analysis for reducing vibration and noise. Researchers studied methods to analyse acoustic emission of the gearbox structure under the time varying stiffness, major excitation on component level, and a new method was presented to reduce the vibration and noise. Transfer path analysis between the source of noise and the emission to the customer in a vehicle is a field that most researchers have focused on since 90's and it is mainly used to find the root cause of a noise problem in a vehicle and find the transfer paths that are relevant to the problem. Transfer path analysis (TPA) is the classic method used to evaluate and determine the relationships between the inputs (vibration or sound source) and the received outputs; various TPA methods can be used, to calculate the transfer functions. Different types of them have their own advantages and disadvantages so the application dictates which is the best one for the job. For example, TPA is not quicker and has some limitations due to the requirement of considering all the paths. Operational transfer path analysis (OTPA) is quicker, but it lacks reliability and is not as accurate. Operational path analysis with exogenous inputs (OPAX) is the most accurate among the others, on the other hand, it needs more time in terms of execution with comparison to the OTPA (Diez-Ibarbia, A., et al 2016).

Since there is a development trend of hybrid and electric vehicles, the focus of the project will be on these two categories of vehicles. Especially for battery electric vehicles, the acoustic quality is an elementary factor, noises of the auxiliary components and the electrified powertrain are more perceived in the vehicle cabin. (Albers, A., et al 2014).

In hybrid vehicles, since the IC engine is inactive in the pure electric phase, depending on current drivetrain status (IC is active or inactive), they share the same NVH problems with the EV and the IC vehicles. In addition, there are the enormous number of elastic and rigid components in hybrid electric vehicle (HEV) which cause various NVH characteristics and problems in the entire system or individual parts, so NVH behaviour of these types of powertrains are different from ICE vehicles (Qin, Y., et al 2020).

The NVH behaviour of the HEVs powertrain by developing dynamic models has been studied widely, to determine the noise and vibration characteristics of powertrains (Jian Jiang, X., et al 2012; and Zhang, L., et al 2018).

Based on reviewing the research, there is a gap to focus on the NVH optimization of the vehicle to increase the comfort of passengers, while at the same time considering lightweight design. Lightweight design of modern vehicles is an accepted procedure to reduce the energy consumption and can have effect on acoustic behaviour, by changing sound transmission or shifting of resonances into operating ranges (Hau, X., et al 2021). Since in the current models only sound-pressure level or the respective frequency spectrum is considered, it is necessary to consider the complete vehicle level and analyse the noise with psycho-acoustic metrics to consider the human perception.

Research Method:

Reducing noise and vibration of vehicles is the desired goal to achieve; however, the optimization by purely considering the level of noise pressure reaches its limits due to the weight–noise optimization problem. The potential of a psychoacoustic based approach by utilizing psychoacoustic metrics to decrease the negative impact of these acoustical phenomena have not yet been researched sufficiently. Investigation of the NVH effects caused by lightweight design choices in the vehicle powertrain and development of metrics to best

identify annoying components of generated noise and vibration are the research gaps in this field.

Developing a test-based method for noise optimized gearboxes, by considering lightweight specifications and psychoacoustic metrics, is the main purpose of this project. The possible design parameters for lightweight gearboxes and their impact on acoustical behaviour will be extracted. The acoustic and vibrational behaviour will be derived, and then further analyzed to quantify psychoacoustic properties at the driver position.

In the first step, identifying the relationship between psychoacoustic parameters and human comfort will be the focus. By calculating the selected human comfort indices, a method to extract the relationship between vibro-acoustic signals and human comfort indices will be proposed. Identifying the effect of gearbox design parameters on the NVH results of the gearbox in the cabin is the aim of the next step. Gearbox model will be developed and simulation on the vibro-acoustic behaviour of the model in a suitable software will be done. The results of this step will help us to narrow down the most relevant design parameters regarding to improve the vibrational behaviour. Simulation with a lightweight transmission system will be conducted to investigate how the acoustical behaviour is altered due to its lightweight design. The research will be continued to propose suggestion, recommendation, and modification for NVH testing. Relevant NVH standards and test routines for the vehicle gearbox will be studied in detail to compare them. At the last step, a test based on the proposed method will be conducted on the components as real test object. The test will be performed in both standard routine and proposed routine to make a comparison between their results. Additionally, if vehicle will be available to be tested a transfer path analysis will be conducted, to quantify the most dominant transfer paths and frequency response functions from the gearbox to the driver ear and their influence on the in-cabin noise of the vehicle. Furthermore, we want to conduct measurements on the component level with gearboxes for electrical drives in a XiL-Framework, to build up experience and identify the impact of design parameters on NVH behaviour.

By comparing and evaluating different test methods, we can identify the most efficient methods, and increase effectiveness of extracting psychoacoustic metrics of lightweight gearboxes even from component testing. Comparing the results of experimental approach and numerical one will be proper validation for providing an accurate final method. The developed method will serve as a tool for optimizing the vehicle-development process.

3.2 ESR6 - Sensitivity analysis of lightweight design concepts in terms of gearbox acoustics

The total sound power level of a gearbox under gear mesh excitations can be given as:

$$L_w(f) = L_F(f) + L_{hT}(f) + L_s + L_\sigma(f)$$

Where L_f is referenced to the excitation level (N), L_{hT} to the gearbox transfer admittance ($ms^{-1}N^{-1}$), L_s to the enveloping surface (m^2) and L_σ to the dimensionless radiation index (Linke, et al 2016).

This decomposition of is planned to be studied in a virtual approach using simulations coupling MBD and FEM/BEM techniques. A main task is the development of a virtual analysis package which predicts the dynamic behaviour of different subsystems in a gearbox. A multibody simulation package using Simpack can help model gear contact, predict gear mesh excitations and the consequent structural response of a gearbox. The surface velocities of the gearbox are then used to predict the radiated noise in an acoustic package in ANSYS.

The components can be modelled in a CAD environment or created through primitive geometries available in Simpack. To capture correct system dynamics, the components need to be represented as flexible bodies in the multibody simulation environment. Gearbox housings are often modelled as rigid bodies in multibody simulations but their flexibilities cannot be ignored for designs optimised for light structures. Completely different NVH behaviours have been observed in studies that compare the influence of rigid housings and flexible housings in wind-turbines. (Vanhollebeke F.; et al, 2012)

Similar studies also highlight the effect of using rigid shaft and flexible representation of shaft elements on gear-train modes. (Helsen, Jan et al, 2010) As a general rule, any component with significant modal content within the frequency range of interest needs to be modelled as a flexible component in multi-body analysis.

Since direct FE models are computationally demanding on the simulations, reduced representation can be prepared using the Craig-Bamton method (Craig R, Bampton M, 1968). The frequency range of the excitation content (mesh frequency) determines the amount of modes that are considered during the reduction of FE models.

The components are then assembled and the model is run with a time integration solver. It is possible to extract key structural results like transmission errors at the gear meshes, bearing loads, excitation at bearing seats at this stage. In case of flexible housings, surface velocities can also be computed using recovery matrices linked to the reduced representations of the gearbox housing models. The surface vibration is then used to calculate the airborne sound using boundary element method in a separate acoustic package in ANSYS.

All these extracted nodal result elements can be analysed separately to study component dynamics, or together to see the relative contribution of sub-system group to the overall NVH character of the gearbox. Identification of key contributing elements then help in component-focused design improvements. Several studies on such targeted improvements are available in the literature, some of which are discussed in the paragraphs that follow.

Shadi Shweiki et al investigated gear-pair models combining nonlinear FE simulations and lumped-parameter modelling to study the mass reduction effects on the dynamics behaviour of spur gears (Shadi Shweiki et al, 2017). The study revealed the influence of reducing blank stiffness and geometry-periodic material removal from gear blanks on the dynamic transmission errrors. Hensel, Eric et al used a frequency-based substructuring method to check the acoustical behaviour of gearboxes with various gear blanks. Several novel gear blank forms were analysed including a gear with an innovative metal foam core developed at Fraunhofer IWU (Hensel, Eric et al 2021)

In a 2018 study, Zhou et al executed housing optimizations for a double planetary gear system (Zhou, Weijian et al, 2018). Acoustic contributions from different gearbox panels were evaluated and the key radiation surface was chosen to be equipped with stiffening ribs. Using a response surface method (RSM) running with parametric structural design variables for the ribs, significant reductions were observed in select frequency ranges of interest. The study shows promising control possibilities over the acoustic radiation of the gearbox housing.

In addition to geometry modifications, another front of development is the exploration of alternative material selection in the design of gearbox components. Figlus, Tomasz et al experimented with several composite-materials for their vibro-acoustical performance as alternatives for gearbox housing material. It was found that although their dynamic response was higher than a reference steel housing below 1 kHz due to resonant frequencies, there was a significant reduction in the acoustic repose in the frequency span above 1 kHz. A glass mat reinforced composite configuration in the study exhibited an acoustic level reduction of over 15 dB in frequencies above 4 kHz. Additional testing is required to evaluate long life-cycle use these alternative materials but further research on their use in gearbox housing designs has been advised. (Figlus, Tomasz, 2019)

In light of the multibody simulation capabilities available at hand and key literature presenting state of the art in simulation methods and future design possibilities, this ECO drive activity is focusing on simulation based sensitivity studies for new lightweight design concepts for gearboxes. A vibro-acoustic simulation chain is being prepared and refined with checks on a sample gearbox geometry. The use of this methodology will be extended on a commercial gearbox for insights into its NVH behaviour. Novel part designs and the use of acoustically promising materials (e.g. metal foam structures and metamaterials) can then be explored as potential design improvements.

5 Bibliography

Maier, T 2011, A Contribution to the Generation of Complex Structure Dynamic Simulation Models and their Validation by 3D Laservibrometry. PhD thesis, Karlsruher Institut für Technologie (KIT), Karlsruhe,

Jian Jiang, X., Ju-hua, H., Qun, L., Study on vibration and noise of hybrid electric vehicle', Future communication, computing, control and management. Springer; 2012. p. 373–382.

Albers, A., Fischer, J., Behrendt, M. and Lieske, D., Identification and definition of acoustic relevant limit values for electric vehicles. Internationales Stuttgarter Symposium, 2014.p. 1339-1354.

Diez-Ibarbia,A., Battarra, M., Palenzuela, J., Cervantes, G., Walsh, S., De-la-Cruz, M., Theodossiades, S., and Gagliardini, L., Comparison between transfer path analysis methods on an electric vehicle. Applied Acoustics, 2016.

Fischer, J 2017, Methods for the Validation of Electric Vehicle Interior Noise with Regard to Tonal Noise due to Torsional Excitation by the Electric Drive. PhD thesis, Karlsruher Institut für Technologie (KIT), Karlsruhe,

Zhang, L., Chen, W., Meng D, and Peng G, Yu Z. Vibration analysis of series-parallel hybrid powertrain system under typical working condition and modes. Technical Report. SAE Technical Paper; 2018.

Qin, Y., Tang, X., Jia, T., Duan, Z., Zhang, J., Li, Y., and Zheng, L., Noise and vibration suppression in hybrid electric vehicles: State of the art and challenges. Renewable and Sustainable Energy Reviews; 2020.

Hua, X., Thomas, A., and Shultis, K., Recent Progress in Battery Electric Vehicle Noise, Vibration, and Harshness. Science progress, 2021, vol. 104(1) 1-11.

Linke, Heinz; Börner, Jörg; Hess, Ralf , Cylindrical gears. Calculation, materials, manufacturing. Cincinnati Ohio: Hanser; 2016

Vanhollebeke F.; Helsen J.; Peeters J.; Vandepitte D.; Desmet W., Combining multibody and acoustic simulation models for wind turbine gearbox NVH optimisation. Proceedings of ISMA 2012

Helsen, Jan; Vandepitte, Dirk; Desmet, Wim, Flexible modelling of wind turbine gearboxes with special focus on shaft flexibilities, 2010

Craig R, Bampton M, Coupling of substructures for dynamic analysis. AIAA J 6(7):1313–1319, 1968

Shweiki, Shadi; Palermo, Antonio; Mundo, Domenico, A Study on the Dynamic Behaviour of Lightweight Gears. In Shock and Vibration 2017, pp. 1–12.

Hensel Eric, Bräunig Jan, Troge Jan, Stapf Tom, Drossel Welf-Guntram, Efficient evaluation of the acoustical behaviour of gearboxes with various gear blanks using frequency-based substructuring. ICSV27 conference proceedings, 2021

Zhou, Weijian; Zuo, Yanyan; Zheng, Mingyin, Analysis and Optimization of the Vibration and Noise of a Double Planetary Gear Power Coupling Mechanism. In Shock and Vibration 2018.

Figlus, Tomasz; Kozioł, Mateusz; Kuczyński, Łukasz, Impact of Application of Selected Composite Materials on the Weight and Vibroactivity of the Upper Gearbox Housing. In Materials, 2019 (Basel, Switzerland) 12 (16), p. 2517.